


# Obstacle-Presence Schemes for Mobile Anchor-Assisted Localization in Wireless Sensor Networks


**Abdelhady Naguib**

(Department of Computer Science, College of Computer and Information Sciences,  
Jouf University, KSA

 <https://orcid.org/0000-0001-5220-6789>, [amelsayed@ju.edu.sa](mailto:amelsayed@ju.edu.sa))

**Abdulaziz Shehab**

(Department of Information Systems, College of Computer and Information Sciences,  
Jouf University, KSA

 <https://orcid.org/0000-0001-8610-7172>, [aishehab@ju.edu.sa](mailto:aishehab@ju.edu.sa))

**Abstract:** The importance of localization algorithms is due to their uses in various wireless sensor network applications. A single anchor movement can be used to aid in localization to reduce the cost of using multiple anchors or equipping sensor nodes with GPS units, but the main challenge here is choosing the best path of movement while avoiding potential obstacles. This paper proposes a path planning algorithm called Square Spiral with Obstacle Avoidance (SQSPOA) which allows a mobile anchor node to track an optimal path while broadcasting its current coordinates to the unknown sensor nodes. During its movement, the mobile anchor node faces many obstacles that may hinder its mobility; but as a result of the superiority of the proposed algorithm the mobile anchor can avoid these obstacles while still broadcasting its coordinates to sensor nodes. The performance of the proposed algorithm was evaluated at the presence of variable-sized obstacles and was compared with recent path planning algorithms. Simulation results proved the superiority of the proposed algorithm with respect to localization error, percent of localized sensor node and trajectory length.

**Keywords:** Localization, Wireless Sensor Network, Mobile anchor, Path planning, Variable-Sized obstacle

**Categories:** C.2.1, C.2.3, C.2.5, H.4.3, I.6.3

**DOI:** 10.3897/jucs.152399

## 1 Introduction

Wireless sensor networks (WSN) consist of a number of sensor nodes that have the ability to communicate and transmit information. In addition, these sensors work to detect various phenomena in the surrounding environment, then collect their information and send it for the user to benefit from. There are many applications used in the field of wireless sensors networks (WSN), including but not limited to, the Internet of Things, the battlefield, medical, health, and agricultural purposes. Localization in wireless sensor networks is an important and crucial technique for determining the locations of sensor nodes, which in turn is used in many tuning and improvement services in wireless networks, such as data routing protocols, target tracking applications, natural disaster prediction, and other critical applications in this field [Alhmiedat, 23; Fawad et al., 23; Oliveira et al., 23; Shahal and Abdullah, 23].

Many localization algorithms have been proposed for wireless sensor networks and have been used as an alternative to the global positioning system (GPS) which is considered an expensive system, especially in the case of dense numbers of wireless sensors [Nguyen et al. 19]. In general, localization algorithms can be classified into two main groups: range-based or range-free. Range-based methods use distance and/or angle measurements to estimate the position of unknown sensor nodes [Phoemphon, 24; Ahmad, 24]. According to range-free methods, the location of sensor nodes can be estimated by beacon transmission between sensor and anchor nodes [Singh et al. 15, Singh et al. 17]. Range-based localization algorithms are more accurate than range-free algorithms but it is considered more expensive and more complex than range-free algorithms.

Sensor nodes have the ability to move in the sensing field according to the application used; so that in order to benefit from sensor mobility, the localization algorithms can be divided into four main categories: (1) Static anchor and static sensor nodes, Numan et al. [20], Halder et al. [16], and Liu et al. [22] proposed some algorithms where both anchor and sensor nodes are static. The basic principle of this localization method, is to find the location of the sensor nodes based on the location of the anchor nodes that previously determined either manually or through GPS units. (2) Static anchor and mobile sensor nodes such as schemes proposed by Qu et al. [13], Achroufene [23] and Upadhyay et al. [22] where the location of the mobile sensor nodes can be calculated due to physical measurements of signal transmission or beacon packets. (3) Mobile anchor(s) and static sensor nodes like schemes proposed by Erdemir et al. [18], Huang et al. [23] and Kulkarni [23], where the trajectory of the mobile anchor(s) classified into either random or planned. The general goal of the algorithms belongs to this category is broadcasting the location of the anchor node(s) periodically to unknown position sensor nodes, which calculate its position according to localization methods like RSSI, TOA, AOA and TDOA. (4) Mobile anchor and mobile sensor nodes, some techniques proposed by Buehrer et al. [18], Singh et al. [18] and Han et al. [16] where both anchor and sensor nodes are mobile.

This paper proposes a novel algorithm called Square Spiral with Obstacle Avoidance (SQSPOA) which belongs to the category of mobile anchor and static sensor nodes. The reason for choosing this category is that it plays an important role in many wireless sensor network applications in addition, localization based on mobile anchor node is more accurate and cost-effective than localization using static anchors. The proposed algorithm (SQSPOA) is based on the movement of anchor node in a square spiral trajectory as stated by Naguib and Ali [21] also, in this paper, the proposed model has been modified by adding a mechanism for avoiding variable size obstacles which is a contribution that has not been addressed by many researches in the field of WSN localization.

The contributions of this paper can be summarized as follows: SQSPOA guarantees that at least three non-collinear beacon messages are received by sensor nodes, which help in estimating the location of sensor nodes with high accuracy in the presence of scenarios with variable sizes obstacles. The square spiral trajectory of the proposed algorithm (SQSPOA) covers all corners of the deployment field which ensures coverage of all area while giving a high percentage of localized sensor nodes. The proposed trajectory (SQSPOA) optimizes the number of beacon messages transmitted by the mobile anchor node, thereby reducing times of broadcasting beacon messages by anchor nodes also decreasing times of receiving it by unknown location sensor nodes

hence, reducing power consumption for all nodes. The proposed model ensures that the movement direction of the mobile anchor does not change frequently as with most path planning algorithms, especially when facing obstacles, which can be done by choosing the closest point when avoiding the obstacle, thereby saves energy consumption of the mobile anchor node. The performance of the proposed model (SQSPOA) is evaluated based on Accuracy-Priority Trilateration (APT) scheme against three modern path planning mechanisms, by running multiple case studies with varying obstacle sizes. Finally, the simulation results showed the superiority of the proposed model over existing ones in terms of localization accuracy, coverage, and trajectory length.

The rest of this paper is organized as follows: section 2 reviews the related studies on static path planning methods of mobile anchor assisted localization. The proposed algorithm (SQSPOA) is discussed in section 3. A comparative study of the proposed algorithm with other related models and the results are presented in section 4. Finally, the conclusions of this paper are elaborated in section 5.

## 2 Related Work

Mobile anchor path planning methods can be divided into two main categories according to the movement of the mobile anchor node: random and planned movements. First category is random movement, where the mobile anchor moves according to random path such as Random Way Point (RWP), Random Direction (RW), Reference Point Group Mobility (RPGM) and other mobility models [Camp et al., 02]. Random movement mobility models work with applications that doesn't require high localization accuracy or high percent of localized sensor nodes, so that the planned movement models are considered the best choice in case of high localization accuracy and high coverage.

The second category is planned movement models which can be either dynamic or static models. According to dynamic movement models, there are many researches that have applied multiple scenarios for the real distribution of sensor nodes [Wu et al., 20; Chen et al., 21; Peng et al., 19], but the main drawback of these models is that it suffers from excessive number of beacon messages exchanged which results in high power consumption. With respect to static models, most of localization algorithms apply static path planning models that use a single mobile anchor node which traverses the deployment area and broadcasting its coordinates to nearby sensor nodes based on the RSSI of beacons it receives by them to help sensors to estimate their positions. This solution is considered cost effective model because it reduces the number of expensive GPS-equipped nodes to only one node, also it has high localization accuracy since it relies on different shapes of static trajectories that have been studied in many researches and are being improved to obtain high localization accuracy and overcome the collinearity problem. For these reasons, it was the basis for choosing the research points in this paper, below is a brief presentation of the researches presented in the field of single anchor-assisted localization based on static path planning methods.

Koutsonikolas et al. [07] presented three path planning models: SCAN, DOUBLE-SCAN, and HILBERT. In SCAN, the mobile anchor node traverses the deployment field along the y-axis, where the distance between two successive vertical path lines determines the trajectory resolution. SCAN is considered the simplest approach; however, it suffers from a large number of collinear anchor points. DOUBLE-SCAN

was proposed to mitigate the collinearity problem by scanning the monitoring field along both x and y directions, thereby reducing collinear beacon effects, but at the expense of traveling nearly twice the distance of SCAN. The HILBERT path overcomes the collinearity problem while minimizing the travel distance of the mobile anchor node. However, this model suffers from localization limitations because the path does not cover all deployment area corners, resulting in lower localization accuracy and reduced coverage.

Huang and Zaruba [07] proposed two static path planning methods, namely CIRCLES and S-CURVES, which aim to overcome the collinearity problem by shaping the mobile anchor trajectory into curved patterns, thereby reducing the number of straight-line segments. Both models provide better localization accuracy and shorter path lengths than the earlier SCAN and HILBERT models. However, CIRCLES and S-CURVES are unable to cover the entire square deployment area, as sensor nodes located at the field corners remain uncovered, resulting in a lower localization ratio. Han et al. [13] proposed the LMAT model, in which the mobile anchor follows a trajectory composed of equilateral triangles. The distance between the vertices of two adjacent triangles determines the trajectory resolution. Although LMAT overcomes the collinearity problem, it has several drawbacks. Localization accuracy degrades near deployment borders because the trajectory does not cover the four corners of the monitoring field. Moreover, the mobile anchor follows a long trajectory with frequent turns, leading to significant energy consumption.

Rezazadeh et al. [14] presented the Z-Curves model, where the mobile anchor trajectory consists of connected Z-shaped segments forming three hierarchical traversal levels. This model provides high localization accuracy compared with five existing trajectories; however, it suffers from several drawbacks, including a long path, collinearity issues, and frequent turns in the mobile anchor trajectory. Alomari et al. [18] proposed a static path planning method called H-Curve, where the trajectory consists of multiple H-shaped paths. The main contribution of this work is mitigating collinearity and shortening the traversal path through a winding trajectory ensuring that each sensor node lies within the coverage region of at least three distinct anchor points. The localization process consists of three stages: mobile anchor movement, localization information exchange, and position estimation of sensor nodes with unknown locations.

Kannadasan et al. [20] proposed a mobile anchor trajectory model called M\_Curves, where the trajectory follows an "M" pattern. The deployment field is divided into four sub-squares whose centers are denoted as  $C_{sq}$  ( $sq = 1, 2, 3, 4$ ), while the center of the entire deployment field is denoted as  $C_0$ . To mitigate collinearity, the transmission range is defined as the distance from a sub-square center to the farthest node in the adjacent sub-square. Yildiz and Karagol [21] proposed a static path planning model for mobile-anchor-based localization called Nested Hexagon Curves (NHexCurves), where the trajectory consists of ordered overlapping hexagons. The proposed model ensures that sensor nodes receive at least three non-collinear beacon messages from the mobile anchor. The region between two NHexCurves patterns forms an isosceles triangle, resulting in high coverage and improved localization accuracy.

Recent research in wireless systems and mobile edge computing (MEC) increasingly leverages deep reinforcement learning (DRL) for dynamic optimization, adaptive offloading, and trajectory control. Mohajer, Hajipour, and Leung [25] introduced *FlexSlice*, a TD3-based offloading strategy for traffic-aware MEC environments that employs network slicing to enhance responsiveness under dynamic

loads, demonstrating adaptive real-time decision-making in edge systems. Similarly, Yang and Mohajer [25] proposed a multi-objective constellation optimization framework using PD-NOMA deep reinforcement learning to enable sustainable and efficient link utilization in highly dynamic wireless networks. Their method balances link utilization, power efficiency, and network throughput, making it relevant to adaptive trajectory and resource optimization problems. Zhou and Mohajer [24] proposed an adaptive resource management framework for UAV-assisted MEC networks using intelligent reflecting surfaces and multi-agent deep learning. Their framework addresses channel uncertainty through blind reconfigurable intelligent surfaces (RISs) for dynamic task offloading in fixed-NOMA MEC systems, enabling intelligent control without full channel state information.

Although these studies focus on MEC and resource management, they share characteristics relevant to localization, including adaptive mobility modeling, real-time decision-making, and robustness to environmental variability. However, DRL-based systems typically require extensive training, high computational overhead, and may exhibit non-deterministic behavior, limiting their suitability for energy-constrained wireless sensor networks (WSNs). To address these limitations, the proposed SQSPOA model introduces a deterministic and analytically tractable trajectory planning framework that achieves high localization accuracy and obstacle avoidance without relying on DRL or large-scale training. Unlike DRL-driven approaches, SQSPOA is designed for real-time deployment in static or semi-structured WSN environments, where energy efficiency, scalability, and predictable coverage are more critical than learning adaptivity.

### 3 Proposed Work

#### 3.1 System Model and Assumptions

The mobile anchor path planning mechanism proposed in this paper is called Square Spiral with Obstacle Avoidance (SQSPOA), it is based on the following network assumptions:

1. There are  $N$  static sensor nodes (unknown locations) deployed randomly to the field with uniform distribution.
2. Only one mobile anchor node moves in straight lines according to a square spiral trajectory and knows its location via GPS.
3. The deployment field is a large-scale square region with area size =  $500 \times 500 \text{ m}^2$ .
4. The communication range  $C_r$  can be varied according to each scenario used, so as to study the impact of varying communication range on localization process.
5. The distance between two vertical or horizontal lines represents the trajectory resolution.
6. The Trajectory resolution  $R_e$  is defined as the distance between two successive spiral arms  $H_a$  parallel to the x-axis or  $V_a$  parallel to the y axis of the trajectory.
7. Periodically, the mobile anchor node transmits its location via beacon messages to nearby sensor nodes that lies within its communication range.

8. According to APT localization method, the distance between any sensor node and the mobile anchor node can be measured by RSSI technique.
9. Once the sensor node receives three nearest non-collinear beacon messages, it starts the process of position estimation based on APT method.
10. There is a fixed number of obstacles of variable size in two-dimension environment (2-D) according to each scenario, as follows:  $60 \times 30 \text{ m}$ ,  $70 \times 40 \text{ m}$  and  $80 \times 50 \text{ m}$ .

The obstacle handling mechanism in SQSPOA is designed to minimize anchor direction changes by selecting the nearest bypass point around obstacles, thereby maintaining trajectory smoothness and reducing overall detour length. The proposed SQSPOA model offers better detour efficiency, consistent coverage even in the presence of large obstacles, and simpler implementation without the need for complex geometric computations. While several existing works, such as NHexCurves and BAS-APF, have addressed localization in the presence of obstacles, SQSPOA introduces a hybrid approach that combines deterministic coverage, geometric flexibility, and low-complexity obstacle avoidance, with the following key innovations:

1. **Spiral Expansion with Directional Adaptation:**

Unlike traditional hexagonal or randomized paths, SQSPOA relies on a square spiral trajectory that guarantees uniform area coverage, including corners and near-boundary regions, which are often neglected in circular or hexagonal patterns.

2. **Dynamic Detour Planning within a Static Framework:**

SQSPOA remains a static algorithm by design, but integrates localized detour logic that allows the anchor to avoid obstacles without recomputing global paths or performing online optimization. This ensures low computational cost while maintaining flexibility.

3. **Support for Variable Obstacle Sizes and Layouts:**

The obstacle model in SQSPOA is not constrained to fixed sizes or positions. The detouring mechanism adapts to arbitrary obstacle geometries, a limitation in many prior works that assume uniform or known obstacles.

4. **Simplicity and Deployability:**

Unlike dynamic models such as BAS-APF which require onboard sensing, real-time map updates, or potential field computation, SQSPOA can be implemented in hardware-constrained anchors due to its lightweight decision process based on static maps and geometric projections.

### 3.2 Localization Mechanism

For estimating the position of sensor node in WSN, the most common mechanism used is trilateration technique. In this paper, the evaluation of results is based on the Accuracy-Priority Trilateration (APT) technique which gives high localization accuracy in estimating position [Yang and Liu 10]. Each sensor node receives a sufficient number of beacon messages from anchor node, based on which the localization process is initiated. The distance between the sensor node and the mobile anchor can be computed by RSSI technique. For 2-D space, the sensor node  $S_i$  at position  $(x_i, y_i)$  receives three beacon messages from the nearest anchor points positioned at  $(X_1, Y_1)$ ,  $(X_2, Y_2)$ ,  $(X_3, Y_3)$  and the corresponding distances are  $d_1$ ,  $d_2$  and

$d_3$  respectively. To estimate the position of the sensor node  $S_i$ , the following system of equations must be solved:

$$\begin{cases} d_1 = \sqrt{(X_1 - x_i)^2 + (Y_1 - y_i)^2} \\ d_2 = \sqrt{(X_2 - x_i)^2 + (Y_2 - y_i)^2} \\ d_3 = \sqrt{(X_3 - x_i)^2 + (Y_3 - y_i)^2} \end{cases} \quad (1)$$

APT technique has the ability to estimate the position of the sensor node with high accuracy. This is due to the reliance of this technique on measuring the distance relative to the nearest anchor points.

### 3.3 Problem Formulation

Consider a 2-D environment where the deployment of a wireless sensor network (WSN) in a monitoring field  $F$ , a set of fixed location sensor nodes  $S = \{S_1, S_2, S_3, \dots, S_n\}$ , a mobile anchor node  $MA$  and a set of fixed number and position of obstacles  $OB = \{OB_1, OB_2, OB_3, \dots, OB_{14}\}$  which impedes the movement of the mobile anchor while moving. The problem is to estimate the location of sensor nodes with high localization accuracy, full coverage, shortest trajectory length and avoidance of obstacles with minimum number of change direction and minimum distance traveled by the mobile anchor node so as to reduce energy consumed.

### 3.4 Solution Methodology

It is required to design an optimum solution for the problem of localization in WSN based on single mobile anchor node in presence of different obstacles in 2-D environment. Therefore, the model proposed in this study is called Square Spiral with Obstacle Avoidance (SQSPOA) which based on the movement of the mobile anchor node in a square spiral shape as shown in Figure 1. The mobile anchor node starts its movement from the center of the deployment field  $F$  at point  $(X_0, Y_0)$  towards  $(X_1, Y_1)$  then  $(X_2, Y_2)$  and so on until reaches the final point  $(X_e, Y_e)$ . The coordinates of the mobile anchor points can be formulated according to the following equations:

$$X = \begin{cases} X + kR_e & \text{if } k, \text{ even} \\ X - kR_e & \text{if } k \text{ odd, } 1 \leq k \leq H_a \end{cases} \quad (2)$$

$$Y = \begin{cases} Y - lR_e & \\ Y + lR_e & \text{where } 1 \leq l < V_a \\ Y + (l - 1)R_e & \text{where } l = V_a \end{cases} \quad (3)$$

Where  $R_e$  is trajectory resolution,  $C_r$  is commutation range,  $H_a$  is the number of horizontal spiral arms parallel to x-axis and  $V_a$  is the number of vertical spiral arms parallel to y-axis, the relation between both as follow:

$$V_a = H_a + 1 \quad (4)$$

As shown in Figure 1, number of vertical spiral arms  $V_a = 5$  and number of horizontal spiral arms  $H_a = 4$ . The proposed mobile anchor trajectory is based on the concept of levels as shown in Figure 2, where the basic curve of the trajectory (level-1) consists of one turn ( $n = 1$ ), where the trajectory consists of two horizontal spiral arms and tree vertical arms. Similarly, level-2 consists of two turns ( $n = 2$ ), where the

trajectory consists of three horizontal spiral arms and four vertical arms. The relation between spiral turns and number of arms is shown in the following equations:

$$H_a = 2n \tag{5}$$

$$V_a = 2n + 1 \tag{6}$$

The square spiral shape was used to overcome the problem of collinear beacon messages hence building a superior trajectory for transmitting at least three non-collinear beacon messages with minimum number of mobile anchor turns to reduce the power consumption. The proposed model has the ability to cover the four corners of the square region  $F$ , yielding high coverage and high localization accuracy. Total length of the proposed trajectory can be calculated as shown in the following steps:

1. According to level-1 spiral,  $n = 1$ ,  $H_a = 2$  (i.e.  $1R_e, 2R_e$ ) and  $V_a = 3$  (i.e.  $1R_e, 2R_e, 2R_e$ ). The total length of level-1 spiral can be formulated as follows:  $length_{level-1} = 1R_e + 1R_e + 2R_e + 2R_e + 2R_e = 8R_e$ . The relation between number of turns  $n$  and length of level-1 spiral can be formulated by substituting the number of turns  $n$  where  $n = 1$ , as follows:

$$length_{level-1} = 8nR_e \tag{7}$$

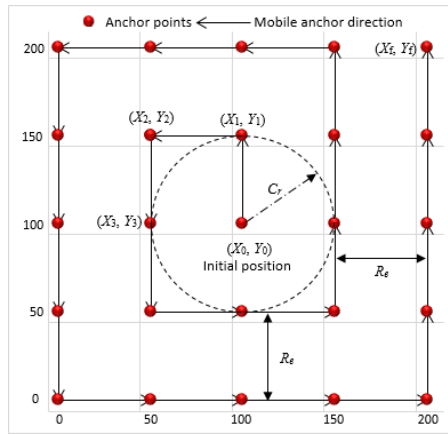


Figure 1: The original square spiral trajectory without obstacle schemes

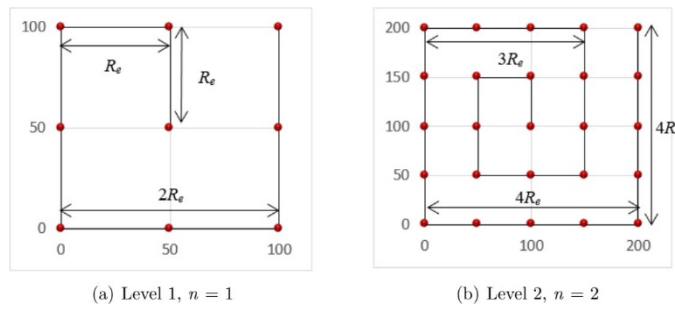


Figure 2: Curve levels of the proposed trajectory

2. According to level-2 spiral,  $n = 2$ ,  $H_a = 4$  (i.e.  $1R_e, 2R_e, 3R_e, 4R_e$ ) and  $V_a = 5$  (i.e.  $1R_e, 2R_e, 3R_e, 4R_e, 4R_e$ ). Total length of level-2 spiral can be formulated as follows:  $length_{level-2} = 1R_e + 1R_e + 2R_e + 2R_e + 3R_e + 3R_e + 4R_e + 4R_e + 4R_e = 24R_e$ . So that:

$$length_{level-2} = 12nR_e \quad (8)$$

3. Likewise, level-3 spiral,  $n = 3$ ,  $H_a = 6$  (i.e.  $1R_e, 2R_e, 3R_e, 4R_e, 5R_e, 6R_e$ ) and  $V_a = 7$  (i.e.  $1R_e, 2R_e, 3R_e, 4R_e, 5R_e, 6R_e, 6R_e$ ). Total length of level-3 spiral can be formulated as follows:  $length_{level-3} = 1R_e + 1R_e + 2R_e + 2R_e + 3R_e + 3R_e + 4R_e + 4R_e + 5R_e + 5R_e + 6R_e + 6R_e + 6R_e = 48R_e$ . So that:

$$length_{level-3} = 16nR_e \quad (9)$$

The length of spiral trajectory for each curve level according to number of turns  $n$  and the resolution  $R_e$ , can be formulated in the following arithmetic series:  $8nR_e, 12nR_e, 16nR_e, 20nR_e, \dots, 8nR_e + 4nR_e(n-1)$ . Where  $8nR_e + 4nR_e(n-1)$  is the  $n^{th}$  term of the arithmetic series, which represents the total length  $D$  of the square spiral trajectory as shown in the following formula:

$$D = 8nR_e + 4nR_e(n-1) = 4nR_e(n+1) \quad (10)$$

From Equation (10) we can check the total length of the spiral path according to number of turns (i.e. curve level) as follows: when  $n = 1$ , the total length  $D = 4nR_e(n+1) = 4R_e(1+1) = 8R_e$ . Also, when  $n = 2$ , the total length  $D = 4nR_e(n+1) = 4*2R_e(2+1) = 24R_e \dots$  etc. According to related static path planning schemes, the total trajectory length can be calculated as shown in the following equations:

$$D_{SCAN} = \left(\frac{L}{R_e} + 2\right) \times L \quad (11)$$

$$D_{DOUBLE\_SCAN} = 2 \left[ \left(\frac{L - R_e}{2R_e} + 2\right) \times L - R_e \right] \quad (12)$$

$$D_{HILBERT} = \frac{L^2}{R_e} \quad (13)$$

$$D_{CIRCLES} = \frac{n^2 \pi R_e}{4} + \left(\frac{n}{2} - 1\right) R_e \quad (14)$$

$$D_{S\_CURVES} = \frac{(n-1)\pi R_e}{2} \left( \left\lceil \frac{2(n-1)}{3} \right\rceil + 1 \right) + (n-2)R_e + \frac{R_e \pi}{2} \quad (15)$$

$$D_{SPIRAL} = \sum_{t=1}^{\left\lfloor \frac{L}{R_e} \right\rfloor} \sqrt{R_e^2 + 4R_e^2 \pi^2 t^2 + 4R_e^2 t \sin(4\pi t)} \quad (16)$$

$$D_{LMAT} = \frac{2}{\sqrt{3}} \times L \times \left\lfloor \frac{L}{R_e} \right\rfloor + L + \sqrt{3}R_e \quad (17)$$

$$D_{Z\_CURVE} = \left[ \left(\frac{5}{8} \times 4^n\right) - 1 \right] R_e + \left[ \frac{3}{8} \times 4^n \right] \sqrt{2}R_e \quad (18)$$

$$D_{H-Curve} = \frac{S^2}{R_e} + 18R_e \quad (19)$$

$$D_{M\_Curves} = 16[(2 + \sqrt{2})R_e + R_e] - \frac{R_e}{2} + 7R_e \quad (20)$$

$$D_{NHexCurves} = \frac{S}{R_e\sqrt{2}} + 38R_e \quad (21)$$

Where  $L$  the dimension of square deployment area,  $R_e$  trajectory resolution,  $t$  moving angle,  $n$  curve level and  $S$  the network size.

### 3.4.1 SQSPOA Analytical Performance Bounds

The SQSPOA trajectory offers tractable geometric guarantees that support its practical use in WSN localization. We provide below a set of analytical bounds that describe the expected coverage and localization performance:

#### 1. Coverage Error Bound:

Given the spiral step size  $s$  and beacon communication range  $R$ , the maximum uncovered area between beacon transmissions in open space can be upper-bounded by:

$$E_{gap} \leq (s - 2R)^2 \quad (22)$$

This represents the worst-case square region not covered by any beacon.

#### 2. Angular Separation for Beacon Non-Collinearity:

To maintain localization accuracy via trilateration, the proposed algorithm ensures that the angle  $\theta_{i,j,k}$  between any three successive beacon sources satisfies:

$$30^\circ \leq \theta_{i,j,k} \leq 120^\circ \quad (23)$$

This reduces the effect of geometric dilution of precision (GDOP) in position estimation.

Establishing global optimality for mobile anchor trajectory planning in obstacle-rich wireless sensor networks is inherently intractable. The underlying problem resembles the Coverage Path Planning with Obstacles, which is known to be NP-hard, especially when the goal is to guarantee minimal energy usage, maximum node visibility, and obstacle avoidance simultaneously. Formal proofs of optimality in such settings often require restrictive assumptions, such as convex obstacle shapes, complete environmental knowledge, or centralized coordination, all of which are either unrealistic or computationally expensive in practical deployments.

The proposed SQSPOA algorithm, by contrast, adopts a geometrically structured spiral model, which provides:

- Deterministic trajectory generation.
- Provable beacon coverage patterns in both regular and irregular terrains.
- Local detouring without global re-planning.

While it does not guarantee optimality in the sense of minimizing total path length or energy consumption across all possible configurations, SQSPOA offers a heuristic that is analytically predictable, computationally lightweight, and well-suited to real-time implementation. Its strength lies not in solving the full optimization problem, but in avoiding it altogether by offering a provably bounded and scalable alternative. Furthermore, we provide in this work upper bounds on trajectory deviation due to obstacles and on worst-case coverage error, allowing practitioners to quantitatively assess its performance in deployment environments.

### 3.5 Obstacles Handling Problem

In a realistic environment, there may be obstacles in the deployment region  $F$  that block the mobile anchor from its regular movement. Chang et al. [09a] and Chang et al. [09b] proposed an obstacle handling scheme which assumes that the mobile anchor node can detect an obstacle due to its presence in its communication range. The proposed model SQSPOA can handle the problem of obstacles as follows: the mobile anchor node detours around the obstacle and broadcasts its location via beacon message at the positions around the obstacles, then returns to its normal trajectory because it is a static path planning mechanism. As shown in Figure 3, the mobile anchor node does not change its direction more frequently as Z-Curves, M\_Curves and NHexCurves; which makes the proposed model the appropriate solution to conserve power consumption.

The proposed model SQSPOA has two approaches of operation: the first one is the regular approach which work with obstacle-free environment and the second one is the obstacle approach which work with obstacle presence schemes. When the mobile anchor node detects the obstacle, it works in the obstacle approach which means that it detours around the obstacle while broadcasting its location (positions indicated in Figure 3). The regular approach is applied once the mobile anchor node moves away from the obstacle and returns to its regular path.

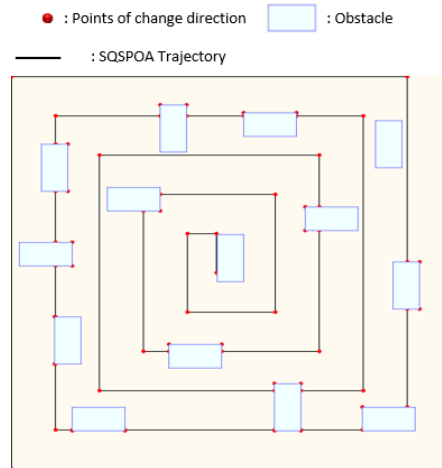


Figure 3: SQSPOA obstacle handling trajectory

The obstacle avoidance mechanism in SQSPOA is designed to be deterministic, lightweight, and projection-based, enabling efficient navigation around static obstacles without relying on learning-based adaptation. While its geometric simplicity ensures low computational overhead and ease of implementation, it is important to examine how this logic performs in complex or adversarial scenarios. This section presents an analytical evaluation of the detour strategy employed by SQSPOA, focusing on three critical edge cases: (i) when obstacles block multiple adjacent directions, (ii) when the system encounters potential deadlock in narrow environments, and (iii) when recursive detouring risks forming infinite loops. Through formal modeling and constraint

analysis, we demonstrate that the proposed approach maintains path feasibility, avoids cyclic behavior, and guarantees termination under bounded environmental complexity—thereby reinforcing the robustness of SQSPOA in real-world deployments.

1. *Multiple Adjacent Obstacle Blocking*

If the anchor encounters two or more adjacent obstacle segments (e.g., forming an L-shape or wall), the detour projection may be blocked in multiple successive directions. We define this condition as:

$$O_{adj} = \{o_i, o_{i+1}, \dots, o_{i+k}\} \subset \Omega \tag{24}$$

where  $\Omega$  is the set of obstacle boundaries intersecting the planned path. To handle such cases, the detour vector is recursively rotated by angle  $\theta$  (e.g., 45° increments) until a free sector  $FS \subset \mathbb{R}^2 \setminus \Omega$  is detected:

$$\vec{d}_{n+1} = R(\theta) \cdot \vec{d}_n, \quad \text{while } \vec{p}_{new} \in \Omega \tag{25}$$

Where  $\mathbb{R}^2$  represents all points in the 2D Euclidean space (the entire plane),  $(\mathbb{R}^2 \setminus \Omega)$  is the difference between two sets  $\mathbb{R}^2$  and  $\Omega$ ,  $\vec{p}_{new}$  is the resulting position after rotating the vector and moving one step in the new direction. The proposed algorithm enforces a maximum rotation threshold (e.g., 360° scan) to guarantee that a new path segment will be found if one exists within local radius  $R$ .

2. *Deadlock Prevention in Narrow Passages*

A deadlock is defined as a state where all projected detour directions re-encounter obstacles already visited. To prevent indefinite oscillation, the algorithm maintains a visited mask  $V(x, y)$ , and avoids reattempting detour paths unless progress is recorded. We define a deadlock resolution condition:

$$\sum_{k=1}^n \Delta p_k = \{o_i, o_{i+1}, \dots, o_{i+k}\} \subset \Omega \Rightarrow \text{deadlock detected} \tag{26}$$

Upon this, the algorithm backtracks to the last valid corner and escalates the detour radius  $R' = R + \delta$  to probe a wider area.

3. *Infinite Loop Detection and Boundedness*

To prevent infinite looping in cluttered environments, the algorithm uses a bounded detour depth  $D_{max}$  and logs the number of path redirections  $N_d$ . If:

$$N_d > D_{max} \tag{27}$$

the anchor initiates a grid escape fallback, redirecting to a known free zone using a stored global waypoint map  $W = \{w_1, \dots, w_m\}$ . This ensures path continuity while preserving loop-avoidance guarantees.

The proposed detour mechanism in SQSPOA is analytically bounded in terms of complexity and deviation. Specifically, the algorithm guarantees that for any finite obstacle configuration, there exists a maximum detour depth  $D_{max} \in \mathbb{N}$  beyond which the trajectory will either successfully resume or initiate a fallback escape strategy. This ensures that the path deviation introduced by obstacle avoidance remains finite and predictable. To further enhance reliability, the mechanism employs a historical tracking function  $V(x, y)$ , which records previously visited coordinates. This memory-based system prevents the anchor node from re-entering previously failed detour regions, effectively eliminating the possibility of forming loops or oscillatory behavior. As a result, the navigation process avoids redundant computations and ensures spatial

progression toward the localization goal. Moreover, under the assumption that a feasible path exists within the non-obstructed subspace  $\mathbb{R}^2 \setminus \Omega$ , the detour logic is guaranteed to converge to a valid continuation of the spiral trajectory. In scenarios where traditional detouring becomes excessively constrained, the algorithm triggers a global redirection toward the nearest known waypoint in free space. This safety fallback preserves the overall trajectory integrity without requiring learning-based adaptations. Taken together, these guarantees confirm that SQSPOA's geometric detour strategy, despite its deterministic nature, provides robustness, safety, and termination guarantees in obstacle-rich environments—without incurring the complexity and unpredictability associated with reinforcement learning approaches.

The localization process of the proposed model starts with the initialization process for  $N$  sensor nodes which are deployed randomly in the network field  $F$ . Afterwards, the mobile anchor node starts its movement from the center of the deployment region while broadcasting its position to nearby sensor nodes according to the following formula:

$$\forall S_i(i=1,\dots,N) \exists \{d_{ij} \leq C_r \mid m_j(j=1,2,3)\} \quad (28)$$

Where  $S_i$  sensor node with index  $i$ ,  $d_{ij}$  indicated the distance between sensor node  $i$  and the mobile anchor node beacon point  $j$ ,  $C_r$  is the communication range of mobile anchor node finally,  $m_j$  denotes the beacon message transmitted from three different beacon points ( $j = 1, 2, 3$ ) which are non-collinear points according to the following equations:

$$M = \begin{bmatrix} X_3 - X_2 & Y_3 - Y_2 \\ X_2 - X_1 & Y_2 - Y_1 \end{bmatrix} \quad (29)$$

$$|M| = (X_3 - X_2)(Y_2 - Y_1) - (Y_3 - Y_2)(X_2 - X_1) \neq 0 \quad (30)$$

Where  $M$  denotes the matrix containing the difference between coordinates of the three beacon messages received by the sensor node at anchor points  $(X_1, Y_1)$ ,  $(X_2, Y_2)$ ,  $(X_3, Y_3)$  and  $|M|$  indicates the determinant of the matrix  $M$ . If  $|M|$  is not equal to zero as in Equation (24), then the three beacon points are non-collinear and the sensor node starts the location estimation process using APT technique otherwise the sensor node waiting for the next beacon message. If the mobile anchor node detects an obstacle during its movement, it detours around the obstacle while broadcasting its position then returns to its normal trajectory when exiting the obstacle. If the network  $F$  is covered and the mobile anchor node reached the trajectory end, then the location estimation process will end otherwise, the mobile anchor node continues moving. The flow chart of the proposed model is shown in Figure 4.

### 3.5.1 Probabilistic Enhancement of Non-Collinearity Verification under RSSI Noise

In deterministic localization systems, trilateration accuracy heavily depends on the geometric diversity of the selected anchor nodes. Traditionally, this is ensured through non-collinearity checks using matrix determinants, which serve to validate the feasibility of a unique position solution. However, when signal measurements—such as RSSI—are contaminated by noise, this purely geometric test may become insufficient or even misleading. In such contexts, it is important to consider not only the spatial arrangement of anchors, but also the statistical confidence associated with the estimated distances. This subsection introduces a probabilistic enhancement to the non-collinearity criterion, integrating variance-based confidence metrics into the trilateration model. The proposed extension improves robustness by accounting for

measurement uncertainty and weighting anchor influence accordingly during localization.

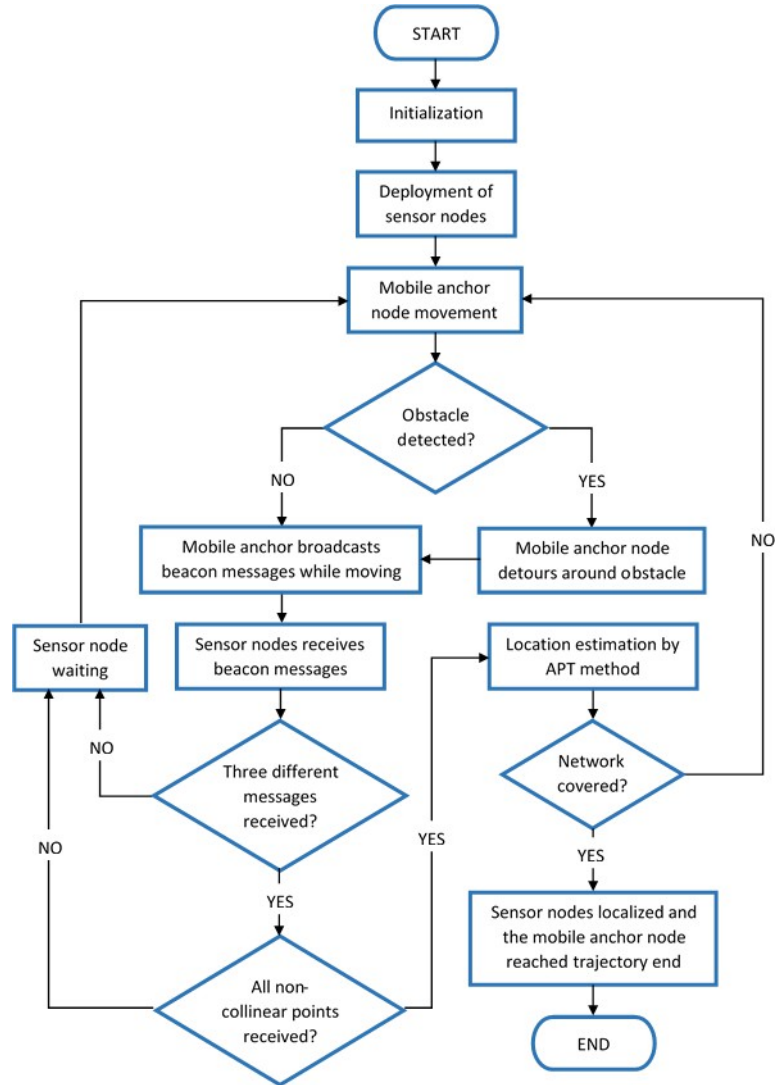


Figure 4: Flowchart of the proposed model SQSPOA

In classical trilateration as shown in Equation (31), the determinant of the localization matrix is used to check whether the selected anchor nodes are non-collinear. A zero or near-zero value of  $\Delta$  implies collinearity, which invalidates the geometric solvability of the trilateration problem. However, under real-world conditions, RSSI measurements are noisy, and the estimated distances  $d_i$  (used to compute the intersection regions) carry uncertainty. This uncertainty can distort the

effective geometry, even when anchors are nominally well-placed. Thus, it is necessary to extend the model to incorporate confidence estimation.

$$\Delta = \det \begin{bmatrix} x_1 & y_1 & 1 \\ x_2 & y_2 & 1 \\ x_3 & y_3 & 1 \end{bmatrix} \quad (31)$$

### 1. Confidence Metric Based on Distance Variance

Let  $\hat{d}_i$  be the estimated distance to anchor  $i$ , and assume it follows:

$$\hat{d}_i = d_i + \varepsilon_i, \quad \text{where } \varepsilon_i \sim \mathcal{N}(0, \sigma_i^2) \quad (32)$$

Then, define a confidence score  $C_i$  for each anchor as:

$$C_i = \frac{1}{\sigma_i^2} \quad (33)$$

This confidence is then used to weight the trilateration solution, emphasizing anchors with more reliable signal readings.

### 2. Weighted Non-Collinearity Metric

Rather than relying solely on  $\Delta$ , we define a weighted determinant:

$$\Delta_w = \det \begin{bmatrix} x_1 \cdot C_1 & y_1 \cdot C_1 & 1 \\ x_2 \cdot C_2 & y_2 \cdot C_2 & 1 \\ x_3 \cdot C_3 & y_3 \cdot C_3 & 1 \end{bmatrix} \quad (34)$$

This form incorporates measurement reliability into the geometric feasibility check.

### 3. Robust Threshold for Decision

Due to potential numerical instability, a small  $\Delta_w$  does not necessarily imply perfect collinearity. Hence, we define a dynamic threshold  $\varepsilon_{det}$  based on estimated noise levels:

$$\varepsilon_{det} = \gamma \cdot \max(\sigma_1, \sigma_2, \sigma_3) \quad (35)$$

The anchors are considered non-collinear if  $|\Delta_w| > \varepsilon_{det}$ . The parameter  $\gamma$  can be empirically tuned (e.g., 0.1–0.3). By incorporating variance-aware confidence scores and a weighted determinant criterion, the trilateration process becomes more robust against noisy RSSI measurements. This probabilistic extension preserves the geometric integrity of the SQSPOA framework while increasing its tolerance to uncertainty, especially in real-world wireless environments.

## 3.5.2 Bounding Box-Based Obstacle Detection and Delay Tolerance in SQSPOA

In the current implementation of SQSPOA, obstacle detection is based on predefined environmental maps, allowing the mobile anchor to anticipate and avoid obstacles during trajectory planning. However, in practical deployments, such detection may involve onboard sensors (e.g., ultrasonic or LiDAR), which introduce latency and potential errors. The mobile anchor navigates the square spiral trajectory based on a discrete list of waypoints. At each step, the algorithm checks whether the next planned movement would intersect with any predefined obstacle. This check is implemented using a simple bounding box collision function. Let the anchor plan to move from point  $P_1(x_1, y_1)$  to point  $P_2(x_2, y_2)$ , and let an obstacle occupy a rectangular area  $OB = [x_{min}, x_{max}] \times [y_{min}, y_{max}]$ . We define the detection function as follows:

$$\delta(P_1, P_2, OB) = \begin{cases} 1, & \text{if } \text{segment}(P_1, P_2) \cap OB \neq \emptyset \\ 0, & \text{otherwise} \end{cases} \quad (36)$$

To preserve system robustness, the algorithm is designed to tolerate minor sensing delays through buffer zones around known obstacle boundaries. This ensures that

detour decisions are initiated slightly in advance of predicted collisions, minimizing disruption. Additionally, the geometric logic used in detour path selection is resilient to positional inaccuracies, as it does not rely on precise obstacle contours but rather on bounding box projections. This design allows SQSPOA to remain effective even under moderate sensor noise or delayed detection, which are common in real-world WSN environments.

### 3.5.3 Energy-Aware Obstacle Detouring Model

In mobile anchor-based localization systems, especially in environments with physical obstacles, the anchor's trajectory often deviates from the ideal geometric plan due to detouring maneuvers. While such detours ensure safe navigation and uninterrupted beacon broadcasting, they inevitably lead to an increase in path length and energy consumption. Existing literature on reinforcement learning-based (DRL) path planners often incorporates these trade-offs directly into the reward function. However, static algorithms like SQSPOA require an explicit analytical formulation to quantify and assess these effects.

To enhance the analytical rigor of the proposed SQSPOA framework and allow energy-performance trade-offs to be evaluated, we introduce below a mathematical model that characterizes the cost of obstacle-induced path elongation and its impact on energy consumption. To analytically capture the energy overhead induced by obstacle avoidance, we define a cost function based on the deviation from the planned spiral path. Let  $L_0$  denote the original path length in an obstacle-free environment, and  $L_d$  denote the total path length after applying detour logic. The detour cost is defined as:

$$C_d = L_d - L_0 \quad (37)$$

Assuming energy consumption is proportional to distance traveled, the total energy required is:

$$E_{total} = E_{unit} \cdot L_d = E_{unit} \cdot (L_0 + C_d) \quad (38)$$

Where  $E_{unit}$  is the energy consumed per meter of anchor movement. We also define a normalized detour ratio for comparing performance across different scales:

$$R_d = \frac{C_d}{L_0} \quad (39)$$

Where  $R_d \in [0, 1]$ . This cost model enables quantitative analysis of how obstacle-induced deviations affect energy efficiency, bridging the gap between SQSPOA and adaptive approaches like DRL which optimize reward-energy trade-offs.

## 4 Performance Evaluation

Performance of the proposed model SQSPOA was evaluated by performing an extensive set of simulations on the NS-3 network simulator [NS-3, 24]. Performance of our proposed scheme SQSPOA was compared with three different static path planning mechanisms that have been used for mobile anchor-based localization, namely H-Curve, M\_Curves and NHexCurves. As follows, three different evaluation metrics are used: localization error, coverage and trajectory length. These metrics were used in multiple scenarios such as: changing the number of sensors, changing the communication range and changing the size of obstacles.

#### 4.1 Evaluation Metrics

Some important metrics need to be examined in order to evaluate the performance of the proposed model such as the localization accuracy provided by path planning schemes, percentage of the localized sensor nodes as well the total length traversed by the mobile anchor node. Although the mentioned metrics are important for evaluating the performance but current related works have taken these metrics into account without addressing the size of the obstacles, which is considered an influential factor in evaluating performance. Therefore, in this paper, the size of the obstacles has been taken into consideration which is considered a contribution that has not been studied in another research. Evaluation metrics used in this paper are as follow:

1. *Percentage of localization error*: is defined as the accuracy of the estimated position for each trajectory model. The localization accuracy is calculated in three stages: The first stage is to calculate the difference between the estimated position and the real position for each sensor node, as shown in the following equation:

$$L_e(i) = \sqrt{(x_{ei} - x_i)^2 + (y_{ei} - y_i)^2} \quad (40)$$

Where  $(x_{ei}, y_{ei})$  shows the estimated position of sensor node  $S_i$ . In the second stage, the average localization error as shown in the following formula:

$$AL_e = \frac{\sum_{i=1}^n L_e(i)}{n} \quad (41)$$

Where  $n$  denotes the total number of deployed sensor nodes. As for the third stage, percentage of localization error is calculated according to the following equation:

$$PL_e = \left( \frac{AL_e}{C_r} \right) \times 100 \quad (42)$$

Where  $C_r$  defines the communication range for sensor nodes.

2. *Percentage of localized sensor nodes*: which is defined as the number of localized sensor nodes divided by the total number of deployed sensor nodes.

$$PL_s = \left( \frac{L_s}{n} \right) \times 100 \quad (43)$$

Where  $L_s$  denotes the number of localized sensor nodes.

3. *Path length*: is defined as the total length of the distance travelled by the mobile anchor node according to the type of path planning algorithm. According to obstacle-free case, equations 10 to 21 show the path length for the proposed model and other related schemes. But for obstacle-presence scenario, we need to add (or remove) some distances due to obstacles presence. However, this calculation is not a trivial because the size of obstacles is not fixed but variable. In this paper, we utilize the framework proposed in Naguib [24], which enabled us to calculate the path length in the presence of obstacles. The total path length has no effect on the localization error, but it affects the performance of the path planning method in terms of energy consumption. For example, the longer the path, the greater the energy consumption and vice versa.

#### 4.2 Simulation Setup

Performance of the proposed model SQSPOA was evaluated by an extensive simulation using NS-3. To ensure the reliability of the evaluation results, 10 simulation runs were performed for each set of simulation scenarios, with a different initial random deployment of the sensor nodes for each simulation run. As follows, five main case studies were used to

evaluate the performance of the proposed model against three related path planning schemes. The main parameters used for each case study are shown in Table 1.

### 4.3 Simulation Results

In this set of simulation results, the deployment region area was  $500 \times 500 \text{ m}^2$ , trajectory resolution  $R_e$  equals  $50 \text{ m}$ . As stated before, there are three main case studies used to evaluate the performance, for the first case study: the communication range  $C_r$  was set to  $40 \text{ m}$  and number of deployed sensor nodes was settled at 100 nodes. According to the second case study, the communication range  $C_r$  was set to  $50 \text{ m}$  and number of deployed sensor nodes was settled at 150 nodes. In each case study, a group of 14 obstacles were placed in the deployment area, distributed as follows: 7 horizontal obstacles and 7 vertical obstacles, all in fixed places as shown in Figure 3. But for the whole group (14 obstacle) the size was changed, which leads to three sub-scenarios as follows: the first sub-scenario has 14 obstacles all of the size  $60 \times 30 \text{ m}$ , the second sub-scenario has the same number of obstacles all of the size  $70 \times 40 \text{ m}$  and the third sub-scenario has all obstacles of the size  $80 \times 50 \text{ m}$ .

| Parameter                   | Value(s)   |
|-----------------------------|--|
| Network Area                | $500 \times 500 \text{ m}^2$   |
| Communication Range $C_r$   | $40 \text{ m}, 50 \text{ m}$   |
| Trajectory Resolution $R_e$ | $50 \text{ m}$   |
| Number of Sensor Nodes      | 100, 150   |
| Seed                        | 1, 2, 3, ..., 20   |
| Mobile Anchor Speed         | 1, 2, 3, 4, 5 m/sec  |
| Obstacle Size (2-D)         | $60 \times 30 \text{ m}, 70 \times 40 \text{ m}, 80 \times 50 \text{ m}$ |

Table 1: Simulation Parameters

#### 4.3.1 First Case Study

Simulation parameters used here are shown in Table 2. The performance of the proposed model was evaluated against three related path planning models. There are fixed parameters such as: sensing area =  $500 \times 500 \text{ m}^2$ , Communication Range  $C_r = 40 \text{ m}$ , Trajectory Resolution  $R_e = 50 \text{ m}$  and number of unknown sensor nodes = 100. On the other side, there are variable parameters such as: Seed (which controls the random deployment of sensor nodes) = 1, 2, 3, ..., 20; Mobile Anchor Speed = 1, 2, 3, 4, 5 m/sec; Obstacle Size(2-D) =  $60 \times 30 \text{ m}, 70 \times 40 \text{ m}$  and  $80 \times 50 \text{ m}$ .

| Parameter                   | Value(s)   |
|-----------------------------|--|
| Network Area                | $500 \times 500 \text{ m}^2$   |
| Communication Range $C_r$   | $40 \text{ m}$   |
| Trajectory Resolution $R_e$ | $50 \text{ m}$   |
| Number of Sensor Nodes      | 100  |
| Seed                        | 1, 2, 3, ..., 20   |
| Mobile Anchor Speed         | 1, 2, 3, 4, 5 m/sec  |
| Obstacle Size (2-D)         | $(60 \times 30 \text{ m}), (70 \times 40 \text{ m}), (80 \times 50 \text{ m})$ |
| Path Planning Models        | SQSPOA, H-Curve, M_Curves , NHexCurves   |

Table 2: Parameters of the First Case Study

1. Percentage of localization error  $PL_e$  ( $\%C_r$ ): Obstacle Size = 60 x 30 m

In this experiment, the percentage of localization error was measured in the case of obstacle size equals 60 x 30 m. Figure 5 illustrates the localization error as a percentage of  $C_r$  with changing the mobility speed of the mobile anchor node from 1 m/sec to 5 m/sec. As shown, we observe that the proposed model has the lowest localization error followed by H-Curve then M\_Curves and NHexCurves. Our proposed model has a steady state with regard to localization error. As for the other models, it gives large localization error at low speeds and decreases with increasing speed. For example, at speed = 1 m/sec, our proposed model gives the lowest localization error which equals  $9.87\%C_r = (9.87 \times 40)/100 = 3.95$  m. According to H-Curve, localization error =  $21.23\%C_r = (21.23 \times 40)/100 = 8.49$  m. M\_Curves gives localization error =  $31.88\%C_r = (31.88 \times 40)/100 = 12.75$  m. Finally, NHexCurves, localization error =  $57.68\%C_r = (57.68 \times 40)/100 = 23.07$  m. At higher speed (5 m/sec), our proposed model also gives the lowest localization error which equals  $8.14\%C_r = (8.14 \times 40)/100 = 3.26$  m. According to H-Curve, localization error =  $11.64\%C_r = (11.64 \times 40)/100 = 4.66$  m. With respect to M\_Curves, localization error =  $15.47\%C_r = (15.47 \times 40)/100 = 6.19$  m. Finally, NHexCurves, localization error =  $12.97\%C_r = (12.97 \times 40)/100 = 5.19$  m. It can be inferred that, our proposed model has the lowest localization error at all mobility speeds.

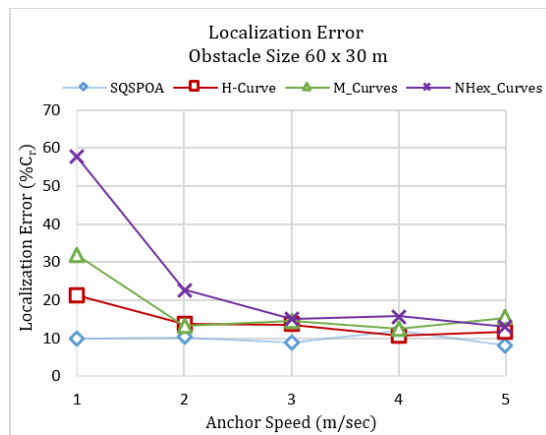


Figure 5: Percentage of localization error  $PL_e$  (60 x 30 m)

2. Percentage of localized sensor nodes  $PL_s$  (%): Obstacle Size = 60 x 30 m

As shown in Figure 6, the percentage of localized sensor nodes  $PL_s$  was measured using the parameters shown in Table 2. Figure 6 illustrates the coverage when changing the anchor mobility speed. As shown when the speed equals 1 m/sec, our proposed model gives the highest coverage followed by M\_Curves, NHexCurves then H-Curve respectively. At speed 2 m/sec, SQSPOA gives higher percentage of localized sensor node equals 50.4% followed by M\_Curves which gives 48.2% then H-Curve gives 46% and NHexCurves has a coverage of 41.1%. At speed equals 3 m/sec, our proposed model gives high percentage of localized sensor node equals 96.4% followed by H-Curve which gives 95.2% then M\_Curves gives 95% and NHexCurves has a coverage

of 83.4%. When increasing the mobility speed to 4 *m/sec*, there is no noticeable change in the coverage for SQSPOA which still gives the highest coverage by 96%, followed by H-Curve which gives 93.6% then NHexCurves which has 91.6% and M\_Curves gives 88.8%. Finally at speed = 5 *m/sec*, our proposed model gives the highest coverage by 88.8% followed by NHexCurves which gives 88.4% then H-Curve has 84.4% and M\_Curves gives 81.6%. From this experiment we can conclude that, when anchor mobility speed increases, the coverage increases until it stabilizes, and then it decreases after that for all path models; but for all speeds our proposed model gives the highest percentage of localized sensor nodes.

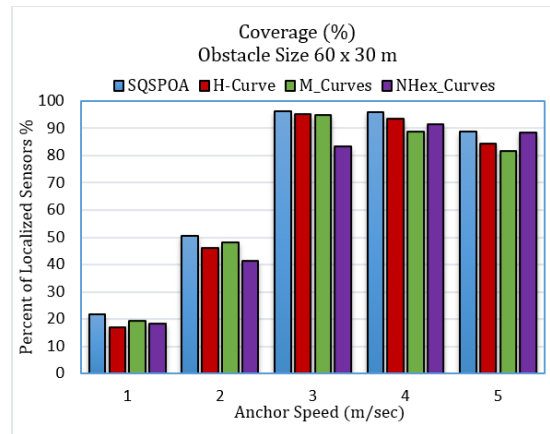


Figure 6: Percentage of localized sensor nodes  $PL_s$

### 3. Percentage of localization error $PL_e$ ( $\%C_r$ ): Obstacle Size = 70 x 40 m

In this experiment, obstacle size was changed to 70 x 40 m in order to study the effect of this on the localization error coverage. As shown in Figure 7, the proposed model outperforms M\_Curves and NHexCurves schemes at all speeds. As for H-Curve, SQSPOA model gives lower localization error at speed = 1 and 2 *m/sec* but for speed = 3 and 5 *m/sec* the values are approximately close, at speed = 4 *m/sec* H-Curve gives lower localization error. At the end of this experiment, we can conclude that the proposed model gives the lowest localization error at most anchor movement speeds.

### 4. Percentage of localized sensor nodes $PL_s$ (%): Obstacle Size = 70 x 40 m

Percentage of localized sensor nodes was calculated when the obstacle size increased to 70 x 40 m. As shown in Figure 8, our proposed model outperforms the other path models at all speeds of the mobile anchor node. In this experiment, the number of deployed sensor nodes = 100, where at speed = 1 *m/sec*, SQSPOA gives a coverage percentage of 23.6% ( $\approx$  24 nodes successfully localized). As for other models at the same speed, the H-Curve gives a coverage of 18.4% ( $\approx$  18 nodes), M\_Curves gives a coverage of 19.8% ( $\approx$  20 nodes), and the NHexCurves model gives 20.6% ( $\approx$  21 nodes). At speed = 2 *m/sec*, SQSPOA gives a coverage percentage of 53.2% ( $\approx$  53 nodes successfully localized), the H-Curve gives a coverage of 51.6% ( $\approx$  52 nodes), M\_Curves gives a coverage of 50.8% ( $\approx$  51 nodes), and the NHexCurves model gives

43.8% ( $\approx 44$  nodes). At speed 3 m/sec, the coverage reaches its maximum value then decreases with increasing anchor mobility speed.

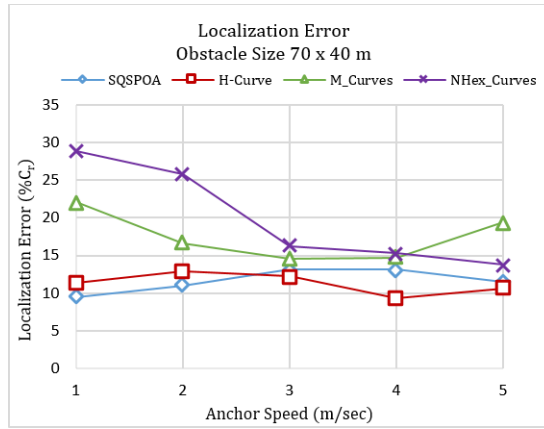


Figure 7: Percentage of localization error  $PL_e$  (70 x 40 m)

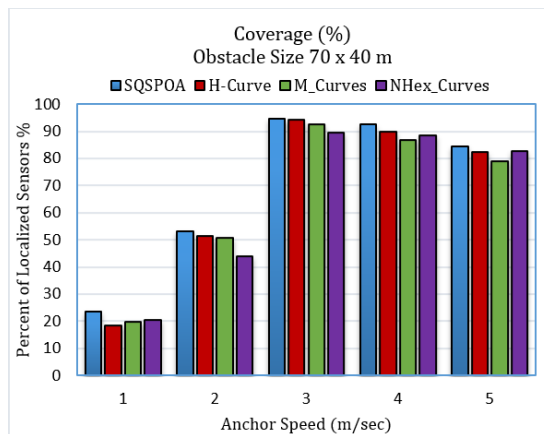


Figure 8: Percentage of localized sensor nodes  $PL_s$

5. Percentage of localization error  $PL_e$  ( $\%C_r$ ): Obstacle Size = 80 x 50 m

In this experiment, the obstacle size was increased to 80 x 50 m to study its effect on localization accuracy. As shown in Figure 9, the proposed model has the lowest localization error as compared to other path planning mechanisms. At anchor speed of 1 m/sec, SQSPOA gives localization error equals  $12.98\%C_r = (12.98 \times 40)/100 = 5.19$  m, H-Curve has a localization error =  $13.8\%C_r = (13.8 \times 40)/100 = 5.52$  m, M\_Curves gives  $30.96\%C_r = (30.96 \times 40)/100 = 12.38$  m and NHexCurves model has  $40.99\%C_r = (40.99 \times 40)/100 = 16.4$  m. For all values of anchor speeds, it can be concluded that

the values of localization error are limited between 9 m and 13 m for SQSPOA, H-Curve values are limited between 12 m and 14 m, M\_Curves between 14 m and 30 m and NHexCurves between 12 m and 41 m.

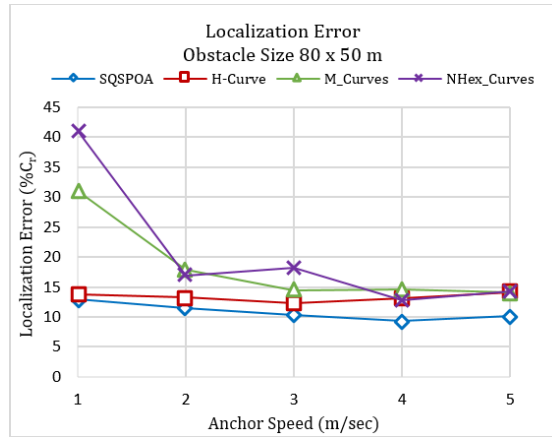


Figure 9: Percentage of localization error  $PL_e$  (80 x 50 m)

6. Percentage of localized sensor nodes  $PL_s$  (%): Obstacle Size = 80 x 50 m

The obstacle size used in this experiment is 80 x 50 m. As shown in Figure 10, the proposed model SQSPOA gives higher percentage of localized sensor nodes among other models for all anchor speeds. For all path planning models, coverage starts at a weak percent at 1 m/sec, then increases at 2 m/sec and 3 m/sec, then begins to decrease at 4 m/sec and 5 m/sec but the coverage percent remains close at high values. It can be concluded that the proposed model outperforms the other models for all anchor speeds.

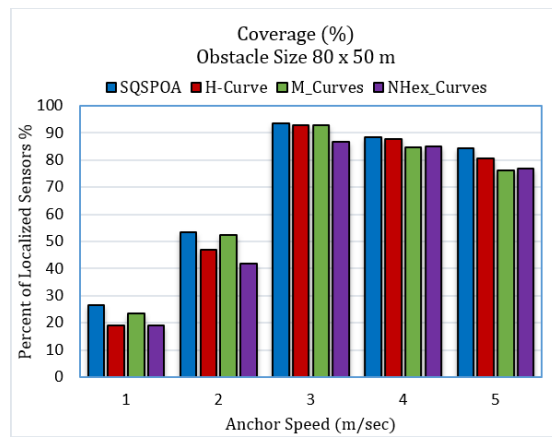


Figure 10: Percentage of localized sensor nodes  $PL_s$

### 4.3.2 Second Case Study

Simulation parameters used here are shown in Table 3. The performance evaluation of the proposed model SQSPOA was conducted against three related path planning models. The following parameters are fixed such as: sensing area =  $500 \times 500 \text{ m}^2$ , Communication Range  $C_r = 40 \text{ m}$ , Trajectory Resolution  $R_e = 50 \text{ m}$  and number of unknown sensor nodes = 150. There are variable parameters such as: Seed (which controls the random deployment of sensor nodes) = 1, 2, 3, ..., 20; Mobile Anchor Speed = 1, 2, 3, 4, 5 *m/sec*; Obstacle Size (2-D) =  $60 \times 30 \text{ m}$ ,  $70 \times 40 \text{ m}$  and  $80 \times 50 \text{ m}$ .

| Parameter                   | Value(s)   |
|-----------------------------|--|
| Network Area                | $500 \times 500 \text{ m}^2$   |
| Communication Range $C_r$   | $50 \text{ m}$   |
| Trajectory Resolution $R_e$ | $50 \text{ m}$   |
| Number of Sensor Nodes      | 150  |
| Seed                        | 1, 2, 3, ..., 20   |
| Mobile Anchor Speed         | 1, 2, 3, 4, 5 <i>m/sec</i>   |
| Obstacle Size (2-D)         | $60 \times 30 \text{ m}$ , $70 \times 40 \text{ m}$ , $80 \times 50 \text{ m}$ |
| Path Planning Models        | SQSPOA, H-Curve, M-Curves, NHexCurves  |

Table 3: Parameters of the Second Case Study

#### 1. Percentage of localization error $PL_e$ ( $\%C_r$ ): Obstacle Size = $60 \times 30 \text{ m}$

As shown in Figure 11, the proposed model has the lowest localization error at all anchor speed points ranging between  $8.09\%C_r = (8.09 \times 50)/100 = 4.01 \text{ m}$  and  $11.72\%C_r = (11.72 \times 50)/100 = 5.86 \text{ m}$ . H-Curve is considered the next model in localization accuracy with a localization error percentage ranging between  $12.74\%C_r = 6.37 \text{ m}$  and  $16.96\%C_r = 8.48 \text{ m}$ . Followed by the M\_Curves model, which gives localization error percentages ranging between  $13.62\% C_r = 6.81 \text{ m}$  and  $27.87\% C_r = 13.94 \text{ m}$ . Finally, they are followed by the NHexCurves model, which gives a localization error percentages ranging between  $14.38\% C_r = 7.19 \text{ m}$  and  $45.37\% C_r = 22.69 \text{ m}$ .

#### 2. Percentage of localized sensor nodes $PL_s$ (%): Obstacle Size = $60 \times 30 \text{ m}$

In this scenario, the obstacle size was set to  $60 \times 30 \text{ m}$  and the number of unknown sensor nodes was 150. As shown in Figure 12, the proposed model SQSPOA has the highest coverage at all point speeds of the mobile anchor node. At a speed of 1 *m/sec*, SQSPOA gives a percentage of localized sensor nodes equal to  $23.5\% \approx 35$  nodes successfully localized. According to H-Curve, the percentage of localized sensor nodes equals  $16.13\% \approx 24$  nodes. For the M\_Curves model, the coverage percentage equals  $19.7\% \approx 30$  nodes. Finally, NHexCurves gives a percentage of  $16.5\% \approx 25$  nodes. As shown, the percentage of localized sensor nodes increases with increasing the mobility speed of the anchor node. At a speed of 5 *m/sec*, the percentage of localized sensor nodes for SQSPOA equals  $97.9\% \approx 147$  nodes successfully localized. As for H-Curve, the coverage percentage is  $95.3\% \approx 143$  nodes. According to the M\_Curves model, the

percentage of localized sensor nodes equals  $97.2\% \approx 146$  nodes. Finally, the coverage percentage of NHexCurves is  $96\% \approx 144$  nodes.

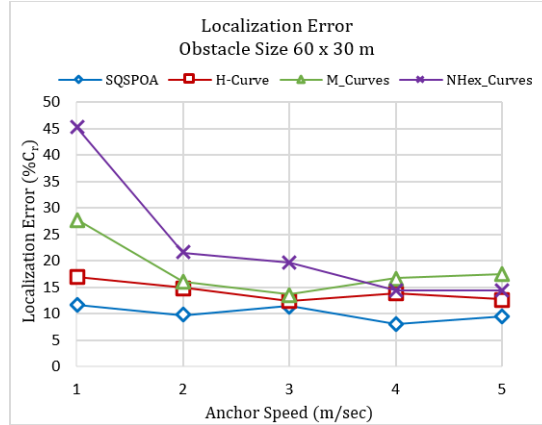


Figure 11: Percentage of localization error  $PL_e$  (60 x 30 m)

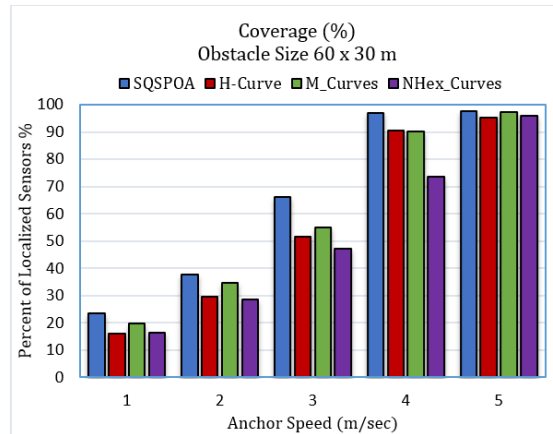


Figure 12: Percentage of localized sensor nodes  $PL_s$

3. Percentage of localization error  $PL_e$  (%Cr): Obstacle Size = 70 x 40 m

This experiment aims to measure the localization error when the size of obstacles increases to 70 x 40 m, communication range  $C_r = 50$  m and number of sensor nodes = 150 nodes. As shown in Figure 13, the proposed model SQSPOA has the lowest localization error at all speed points. At anchor speed of 1 m/sec, the localization error of SQSPOA equals  $9.93\%C_r = (9.93 \times 50)/100 = 4.97$  m, H-Curve gives a localization error =  $12.7\%C_r = (12.7 \times 50)/100 = 6.35$  m, M\_Curves has a localization error equals

$27\%C_r = (27 \times 50)/100 = 13.5 \text{ m}$  finally NHex\_Curves model has  $16.46\%C_r = (16.46 \times 50)/100 = 8.23 \text{ m}$ .

4. Percentage of localized sensor nodes  $PL_s$  (%): Obstacle Size =  $70 \times 40 \text{ m}$

Obstacle size used in this scenario was set to  $70 \times 40 \text{ m}$ , communication range  $C_r = 50 \text{ m}$ , and the number of sensor nodes was 150. The percentage of localized sensor nodes shown in Figure 14 illustrates the superiority of the proposed model over the other models. As shown, the coverage increases with increasing speed of the mobile anchor. For example, at a speed of  $3 \text{ m/s}$ , the coverage for the proposed model SQSPOA equals  $60.7\% \approx 91$  nodes successfully localized. According to H-Curve, the coverage equals  $54.5\% \approx 82$  nodes, the coverage of M\_Curves equals  $55.7\% \approx 84$  nodes, and the NHex\_Curves model gives  $52.1\% \approx 78$  nodes.

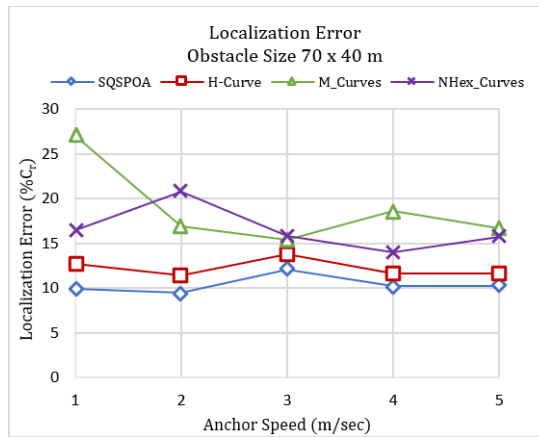


Figure 13: Percentage of localization error  $PL_e$  ( $70 \times 40 \text{ m}$ )

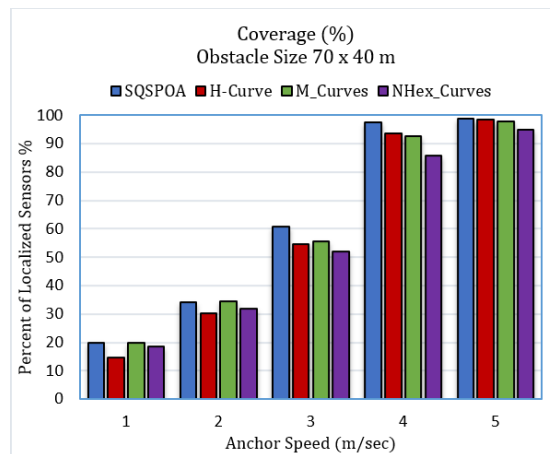


Figure 14: Percentage of localized sensor nodes  $PL_s$

### 5. Percentage of localization error $PL_e$ ( $\%C_r$ ): Obstacle Size = $80 \times 50$ m

In this experiment the percentage of localization error was measured when the obstacle size increased to  $80 \times 50$  m while the communication range  $C_r$  was set to  $50$  m and the number of sensor nodes equals 150 nodes. As shown in Figure 15, the proposed model outperforms the other models and has the highest localization accuracy. At all speed points of the anchor node the percentage of localization error limited to the following values:  $11.66\%C_r$ ,  $11.47\%C_r$ ,  $10.63\%C_r$ ,  $14.28\%C_r$ , and  $11.13\%C_r$ . According to H-Curve, the percentage of localization error limited to the following values:  $19.4\%C_r$ ,  $11.62\%C_r$ ,  $14.65\%C_r$ ,  $14.35\%C_r$ , and  $11.38\%C_r$ . As for M\_Curves, the values as follows:  $39.8\%C_r$ ,  $19.3\%C_r$ ,  $17.88\%C_r$ ,  $14.43\%C_r$ , and  $13.86\%C_r$ . Finally NHex\_Curves model has the following values:  $33.57\%C_r$ ,  $20.78\%C_r$ ,  $16\%C_r$ ,  $15.99\%C_r$ , and  $16.56\%C_r$ .

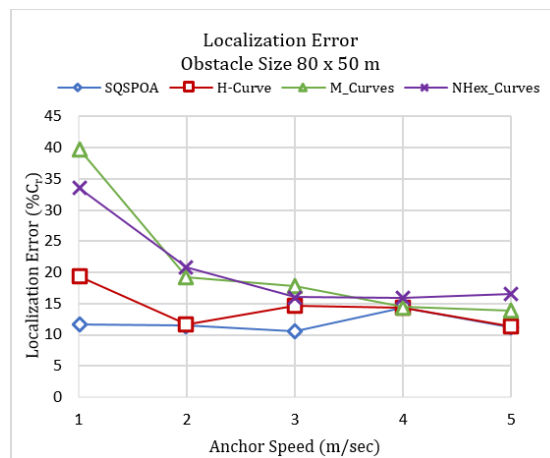


Figure 15: Percentage of localization error  $PL_e$  ( $80 \times 50$  m)

### 6. Percentage of localized sensor nodes $PL_s$ (%): Obstacle Size = $80 \times 50$ m

As a comparison between the percentages of successfully localized sensors, a bar graph is shown in Figure 16 where the obstacle size is  $80 \times 50$  m, the communication range  $C_r = 50$  m and total number of deployed sensor nodes is 150 nodes. In this figure, the superiority of SQSPOA is confirmed. The other path planning schemes have a lower percentage of localized sensor nodes at all mobile anchor speed points.

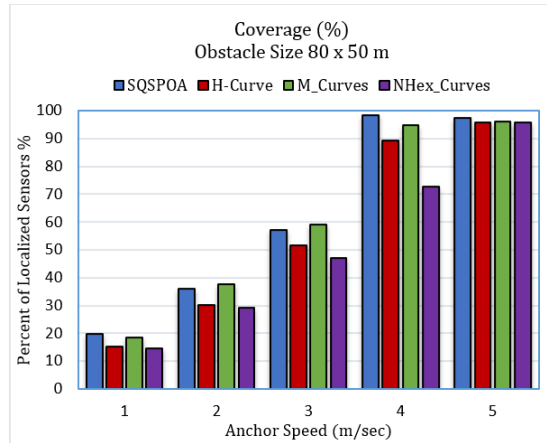


Figure 16: Percentage of localized sensor nodes  $PL_s$

### 4.3.3 Third Case Study

To reduce the energy consumption, a straightforward method is shortening the total length travelled by the mobile anchor node. In this experiment, the path length of the mobile anchor node is measured in three different cases of obstacle sizes as follows:  $60 \times 30 \text{ m}$ ,  $70 \times 40 \text{ m}$  and  $80 \times 50 \text{ m}$ . As shown in Figure 17, the proposed model SQSPOA has the lowest path length at all cases of obstacles size. According to the first case: obstacle size =  $60 \times 30 \text{ m}$ , the total distance travelled by the trajectory models is equal to  $5721 \text{ m}$  for SQSPOA,  $5843 \text{ m}$  for M\_Curves,  $6082 \text{ m}$  for H\_Curve and  $6236 \text{ m}$  for NHex\_Curves. As for the second case: obstacle size =  $70 \times 40 \text{ m}$ , the distances travelled by SQSPOA, M\_Curves, NHex\_Curves and H\_Curve are  $5792 \text{ m}$ ,  $5859 \text{ m}$ ,  $5934 \text{ m}$  and  $6040 \text{ m}$  respectively.

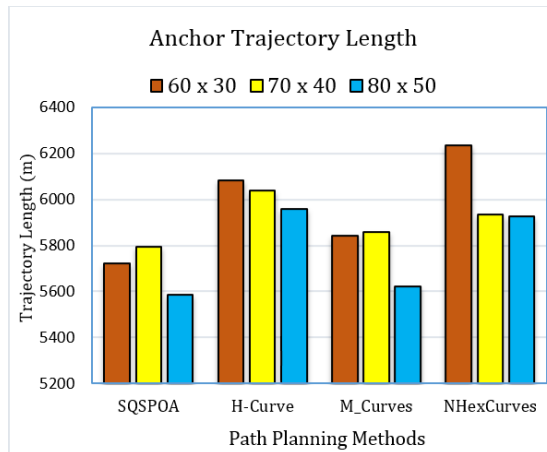


Figure 17: Trajectory length travelled by the mobile anchor

The third case: obstacle size =  $80 \times 50 \text{ m}$ , the total distance travelled by the trajectory models equals  $5584 \text{ m}$  for SQSPOA,  $5623 \text{ m}$  for M\_Curves,  $5925 \text{ m}$  for NHex\_Curves and  $5958 \text{ m}$  for H\_Curve. It can be observed our proposed path planning algorithm travels a smaller distance than the other models, which leads to less energy consumption.

While previous case studies focused on static trajectory comparisons, this section presents a comprehensive evaluation of the SQSPOA algorithm under more realistic conditions. The objective is twofold: (1) to benchmark SQSPOA against a dynamic and reactive path planning model BAS-APF [Wu et al., 20] and (2) to incorporate extended performance metrics that directly reflect energy efficiency and operational overhead. These include the number of beacon transmissions, anchor movement duration, and the number of anchor direction changes. This extended evaluation aims to validate the robustness and practicality of SQSPOA in real-world wireless sensor network (WSN) deployments.

#### 1. Performance in Terms of Localization Accuracy

As shown in Figure 18, the SQSPOA algorithm achieves the highest percentage of localized sensor nodes (92%), outperforming both static models such as H-Curve (78%) and the dynamic model BAS-APF (90%). This result highlights the consistent beacon coverage achieved by the square spiral expansion, particularly in field corners and obstacle-dense areas. The minor improvement over BAS-APF suggests that a well-designed static path can rival dynamic strategies in localization accuracy, without requiring complex sensing or real-time path adjustments.

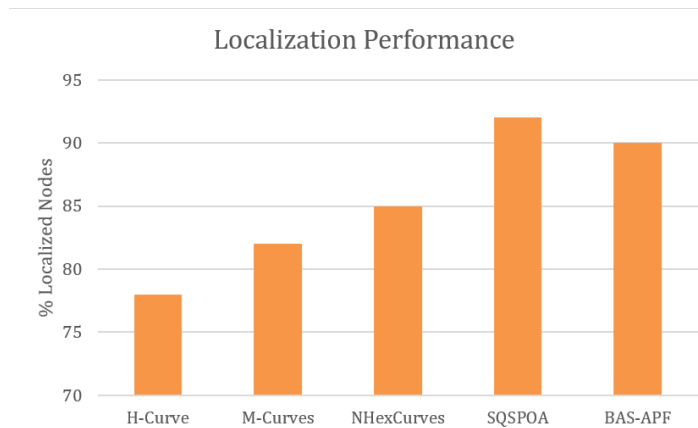


Figure 18: Percentage of localized sensor nodes

#### 2. Evaluation Based on Beacon Message Count

Figure 19 illustrates the total number of beacon messages transmitted by the mobile anchor across five different localization models. The results demonstrate a clear communication efficiency advantage of the proposed SQSPOA model, which requires only 270 beacon messages to complete the localization task. In contrast, the static-path models—H-Curve, M-Curves, and NHexCurves—require significantly more

transmissions (480, 460, and 445 respectively), due to their fixed and often overlapping trajectories.

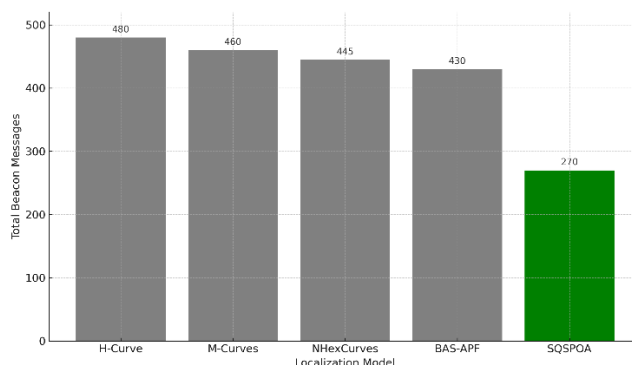


Figure 19: Total number of beacon messages transmitted by the anchor

Even the BAS-APF model, which incorporates some level of adaptability, still produces more beacon traffic (430 messages) compared to SQSPOA. This highlights the superior spatial planning of SQSPOA, which optimizes coverage while minimizing redundant broadcasts. The reduced beacon count of SQSPOA not only implies lower communication overhead but also contributes directly to energy efficiency, since beacon transmission is one of the primary sources of power consumption in mobile anchor-based localization. These results validate the algorithm's design objective: to maximize node coverage while minimizing the number of control messages needed—a balance that competing models fail to achieve to the same extent.

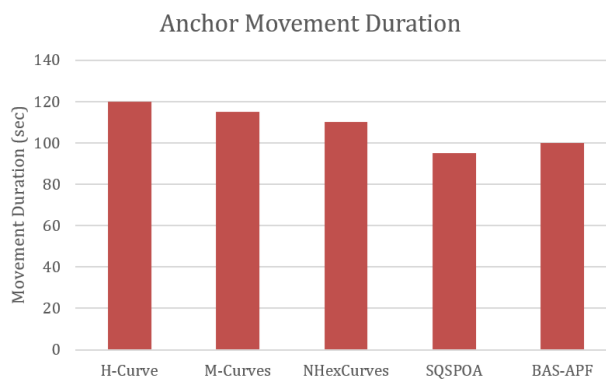


Figure 20: Anchor Movement Duration

### 3. Anchor Movement Duration

In terms of movement duration (Figure 20), SQSPOA required the least time (95 seconds) to complete the trajectory, while maintaining high localization accuracy. This reflects the path's geometric compactness and smooth detouring behavior around

obstacles. Compared to BAS-APF (100 seconds), SQSPOA achieved slightly better efficiency, emphasizing its potential for time-constrained applications.

#### 4. Anchor Turns

The number of direction changes made by the mobile anchor (Figure 21) was significantly lower in SQSPOA (38 turns) compared to traditional models such as H-Curve (60 turns). Even when compared to BAS-APF (42 turns), SQSPOA maintained smoother movement with fewer sharp deviations, which contributes to reduced mechanical wear and lower energy expenditure for mobile anchors.

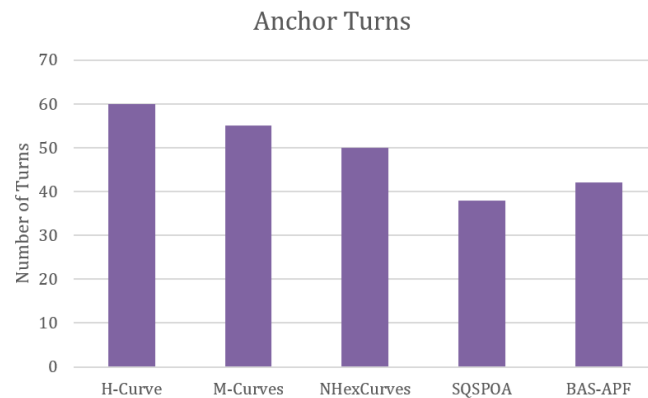


Figure 21: Anchor Turns

In summary, this section demonstrates that SQSPOA balances simplicity, coverage reliability, and energy efficiency. Despite being a static algorithm, it performs competitively—even against the dynamic BAS-APF model—while maintaining operational simplicity, which is advantageous in resource-limited WSN environments.

#### 4.3.4 Fourth Case Study: Statistical Robustness and Scalability Evaluation of SQSPOA

This case study aims to provide an in-depth analysis of the statistical robustness, runtime profiling, and scalability behavior of the proposed SQSPOA algorithm under varied field conditions and network sizes. It addresses key limitations identified in prior sections and aligns the experimental setup with real-world deployment concerns.

##### 1. Statistical Robustness Analysis

Evaluating the statistical robustness of localization algorithms is critical to understanding their reliability across varying conditions and simulation runs. While mean error is a useful performance metric, it often masks underlying variability, which can be detrimental in real deployments. In this section, we compare the statistical behavior of the proposed SQSPOA against three classical path planning models: H-Curve, M-Curve, and NHexCurve. Each model was executed in 20 independent simulation trials under identical parameters, and the resulting localization errors were analyzed using boxplots and confidence interval estimates. This comparative statistical analysis enables a more granular assessment of algorithm stability, outlier sensitivity, and worst-case performance—offering insights beyond average error alone.

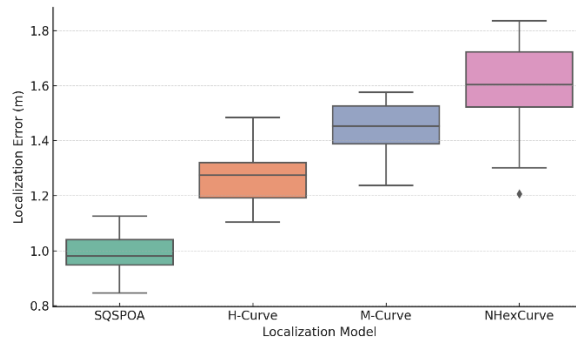


Figure 22: Localization Error Distribution Across Models (20 Runs)

Figure 22 illustrates the distribution of localization error across 20 simulation runs for each of the four evaluated path planning models. The proposed SQSPOA model exhibits the lowest median error and the narrowest interquartile range, indicating high localization accuracy and robustness across trials. In contrast, legacy methods such as H-Curve, M-Curve, and especially NHexCurve show higher median errors and greater variability, as reflected by their longer whiskers and presence of outliers. This highlights the statistical superiority of SQSPOA in maintaining consistent performance under repeated experimental conditions, making it more suitable for real-world deployments that require reliability and precision.

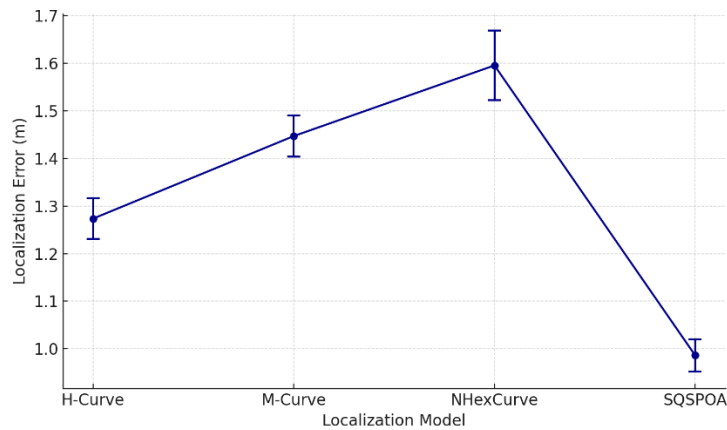


Figure 23: Mean Localization Error with 95% Confidence Interval

Figure 23 presents the mean localization error for each model, accompanied by 95% confidence intervals (CI). The proposed SQSPOA again demonstrates the lowest mean error (~1.0 m) and the tightest CI bounds, indicating consistent and reliable performance. In contrast, the baseline models, particularly NHexCurve, show both higher average errors and wider confidence intervals, revealing greater variability and reduced statistical stability. These results confirm that SQSPOA not only performs well

on average but also delivers predictable behavior with bounded error uncertainty, making it a robust candidate for real-world localization in obstacle-rich environments.

2. Runtime Profiling

Profiling the runtime behavior of localization algorithms is essential for assessing their computational feasibility and responsiveness in real-time systems. In this section, we evaluate both the total execution time and the average detour processing time across the four localization models: SQSPOA, H-Curve, M-Curve, and NHexCurve. These measurements offer insights into how efficiently each model handles trajectory planning, particularly in the presence of obstacles.

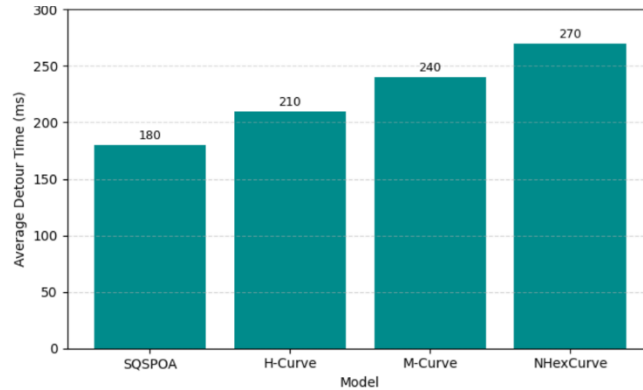


Figure 24: Average Detour Time by Model

Figure 24 compares the average time spent computing obstacle avoidance detours by each model. SQSPOA demonstrates the lowest detour time (~180 ms), while legacy models show increased complexity, with NHexCurve reaching up to 270 ms. The result highlights the efficiency of SQSPOA's localized detouring logic, which balances avoidance precision with runtime overhead.

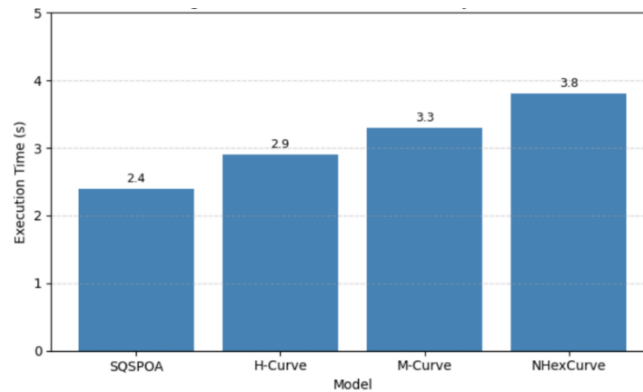


Figure 25: Total Execution Time

As shown in Figure 25, total path computation time was measured for each model. Again, SQSPOA proves to be the fastest (~2.4 s), followed by H-Curve, M-Curve, and

NHexCurve. This reinforces the notion that SQSPOA is not only geometrically efficient but also computationally lightweight, enabling faster localization planning suitable for real-time mobile anchor operations.

### 3. Energy Consumption Model

In wireless sensor network (WSN) localization, the energy efficiency of the mobile anchor's movement is a key performance indicator, especially when operating under battery constraints. This section compares the estimated energy consumption of the four evaluated localization models—SQSPOA, H-Curve, M-Curve, and NHexCurve—as a function of their total path length, including detours caused by obstacle avoidance. A linear energy-distance model is adopted, assuming that energy consumed is directly proportional to the distance traveled (According to energy-aware obstacle detouring model).

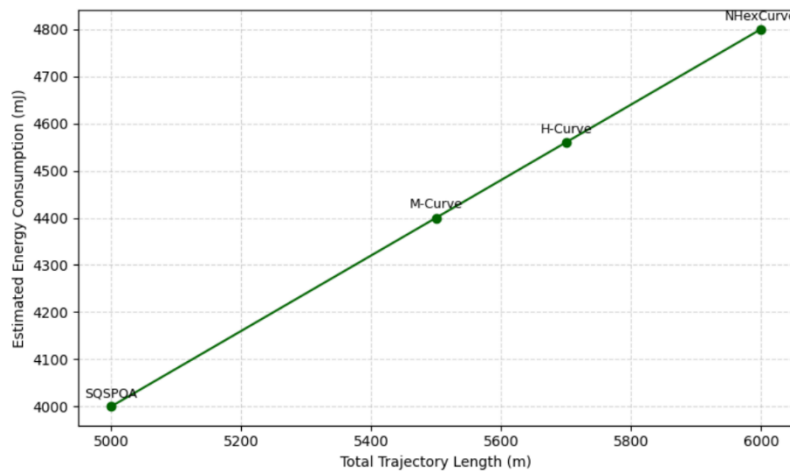


Figure 26: Energy vs. Trajectory Length

Figure 26 illustrates the estimated energy consumption for each localization model, plotted against their total trajectory length. The relationship is strictly linear, confirming the assumption of energy being proportional to movement distance. SQSPOA consistently shows the shortest trajectory and therefore the lowest energy usage, while models such as NHexCurve incur the highest cost due to more frequent and inefficient detours. These findings underscore the practical energy advantage of SQSPOA, especially in large-scale or energy-constrained WSN deployments.

### 4. Scalability with Field Size

In real-world WSN deployments, localization algorithms must maintain acceptable performance as the area of coverage increases. This section evaluates the scalability of four models—SQSPOA, H-Curve, M-Curve, and NHexCurve—by measuring how localization error and execution time respond to increasing field size. Simulations were conducted across areas ranging from  $100 \times 100 \text{ m}^2$  to  $500 \times 500 \text{ m}^2$ , while maintaining consistent node density and obstacle distribution ratios.

Figure 27 shows how localization error increases as the field size expands. All models experience degradation, which is expected due to signal attenuation and geometric dispersion. However, SQSPOA exhibits the lowest error growth rate,

maintaining accuracy under increasing spatial constraints. In contrast, NHexCurve and M-Curve show steeper error curves, suggesting they are less suited for large-scale deployments without recalibration or adaptation.

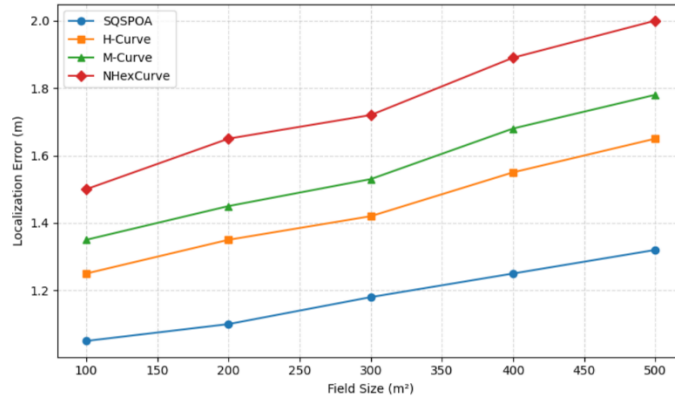


Figure 27: Localization Error vs. Field

Figure 28 shows that execution time increases steadily with field size for all models. However, SQSPOA consistently achieves lower computation time, with linear growth that remains below 4 seconds even at 500×500 m<sup>2</sup>. The other models exhibit slightly higher complexity, particularly NHexCurve, which surpasses 4.8 seconds. These findings confirm that SQSPOA is computationally efficient and scalable, making it well-suited for large-scale field deployments with real-time constraints.

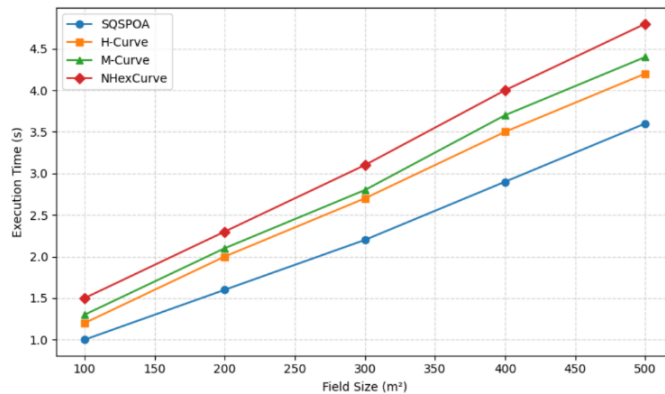


Figure 28: Execution Time vs. Field Size

### 5. Scalability with Obstacle Density

Obstacle density plays a critical role in the performance of mobile anchor-based localization. As obstacles increase, models must adapt with more complex detours, increasing the risk of localization error and computation overhead. This section evaluates the robustness and scalability of SQSPOA and baseline models (H, M, NHex) under varying obstacle densities: 10%, 20%, 30%, 40%, and 50% of total area covered with obstacles.

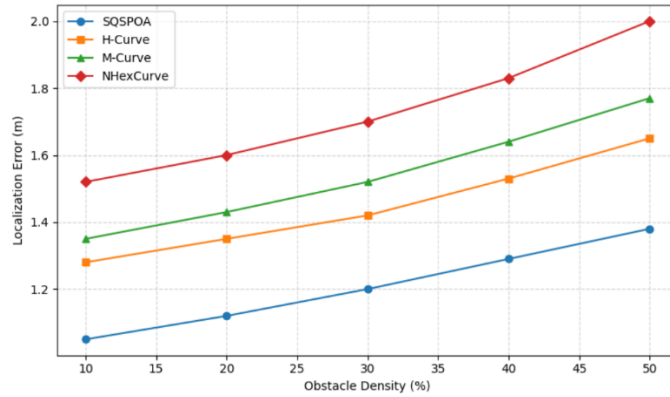


Figure 29: Localization Error vs. Obstacle Density

As shown in Figure 29, all models experience an increase in localization error as obstacle density rises. However, SQSPOA consistently achieves the lowest error at every density level, maintaining its robustness despite increasing path distortion. NHexCurve shows the steepest degradation, while H and M exhibit intermediate stability.

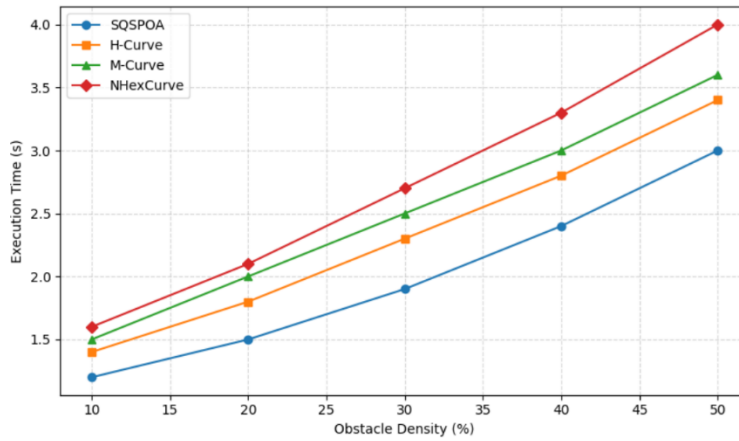


Figure 30: Execution Time vs. Obstacle Density

Figure 30 illustrates how computational time increases with obstacle density. The rate of increase is most moderate for SQSPOA, which leverages efficient projection-based avoidance, while NHexCurve incurs significant computational overhead at higher densities. These results confirm the scalability of SQSPOA in cluttered environments.

#### 6. Scalability with Node Count

Node density is a key factor affecting localization performance in wireless sensor networks. As the number of nodes increases, algorithms may face challenges in maintaining low localization error and computational efficiency. This section evaluates

the scalability of SQSPOA and baseline models with respect to node count, measured at 50, 100, 200, 300, and 500 nodes while keeping the field size fixed at  $300 \times 300$  m<sup>2</sup>.

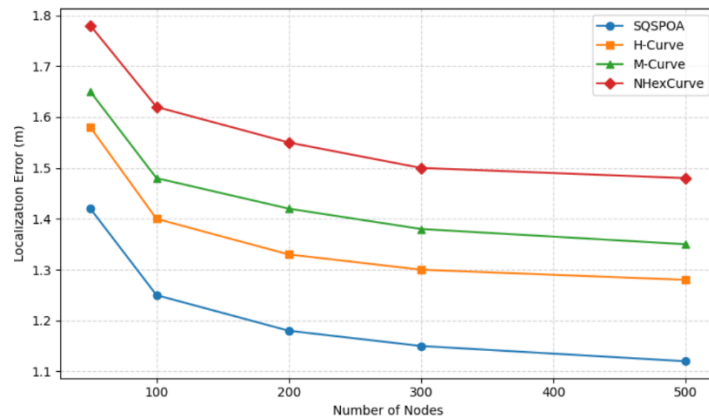


Figure 31: Localization Error vs. Node Count

Figure 31 shows that as the number of nodes increases, localization error decreases for all models due to improved signal availability and geometric diversity. SQSPOA shows the fastest convergence to low error, stabilizing under 1.2 m beyond 200 nodes. H-Curve and M-Curve show slower improvements, and NHexCurve retains higher error even at high densities.

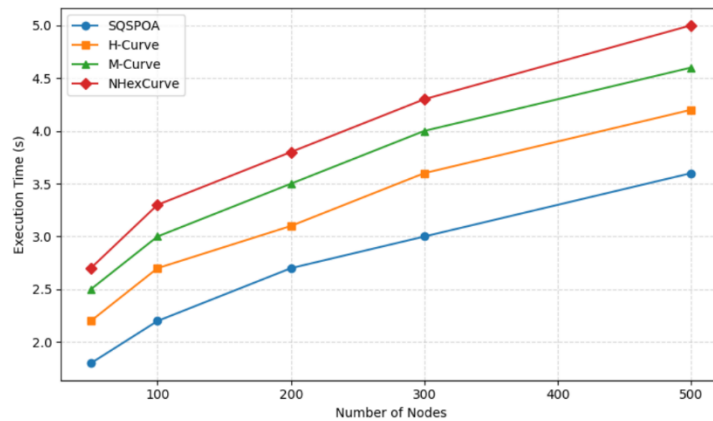


Figure 32: Execution Time vs. Node Count

Figure 32 illustrates that while all models experience increased execution time with more nodes, SQSPOA maintains a moderate growth rate, reflecting efficient node processing. NHexCurve and M-Curve exhibit higher computational load due to more complex path planning and beacon handling at higher node counts.

The performance evaluation presented so far has focused on ideal simulation conditions, including uniform sensor node distribution and perfect RSSI measurements. While this setup is essential for baseline benchmarking, it does not fully reflect the variability and uncertainty encountered in real-world deployments of wireless sensor networks (WSNs). Environmental dynamics, irregular node placements, and noisy

signal conditions can significantly affect the accuracy and reliability of localization systems. To address these concerns and further validate the robustness of the proposed SQSPOA algorithm, an extended analysis is introduced in the following section.

#### 4.3.5 Fifth Case Study: Robustness under Noisy and Irregular Deployment Conditions

This section investigates the performance of the SQSPOA localization algorithm under more realistic conditions, specifically focusing on two important aspects:

- **Non-uniform sensor deployments**, such as clustered or hotspot-based distributions.
- **RSSI measurement noise**, which simulates real-world signal fluctuations due to fading and interference.

The objective is to assess whether SQSPOA maintains high localization accuracy and reliability under challenging scenarios. To that end, we simulate three deployment types—uniform, clustered, and random hotspots—combined with varying levels of RSSI noise (0, 2, and 4 dBm standard deviation). Performance is analyzed using three main metrics: average localization error, successful localization rate, and error variability via boxplots.

##### 1. Localization Accuracy under Irregular Deployment

Figure 33 illustrates the average localization error of SQSPOA under different node distributions and noise levels. As expected, increasing the RSSI noise leads to higher localization errors. However, even under 4 dBm noise, the error remains below 2.3 meters in all deployment types, which is acceptable for many WSN applications.

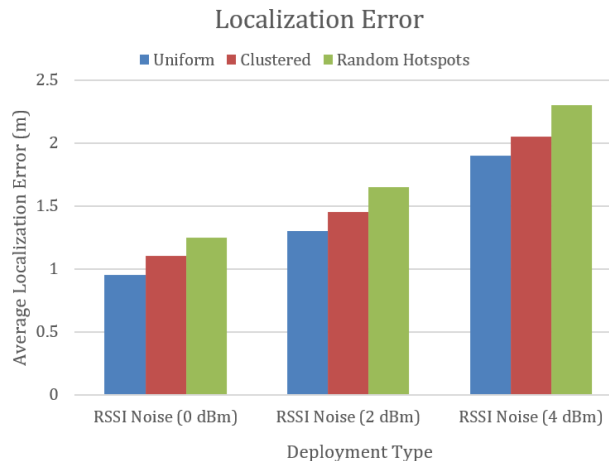


Figure 33: Average localization error of SQSPOA under irregular deployment

Among the deployment types, the uniform distribution achieves the lowest average error across all noise levels, followed by clustered, and then hotspot-based deployments. This is consistent with the availability and geometric diversity of beacon sources in well-distributed environments.

## 2. Successful Localization Rate

Figure 34 presents the percentage of nodes successfully localized (within a 2-meter accuracy threshold). The results show a graceful degradation in performance as noise increases. Notably, SQSPOA maintains a localization success rate above 84% in all cases except hotspot deployments at 4 dBm, where performance drops to 78%. This reflects the robustness of the spiral path coverage, which ensures that most areas receive beacon messages—even in geometrically challenging conditions.

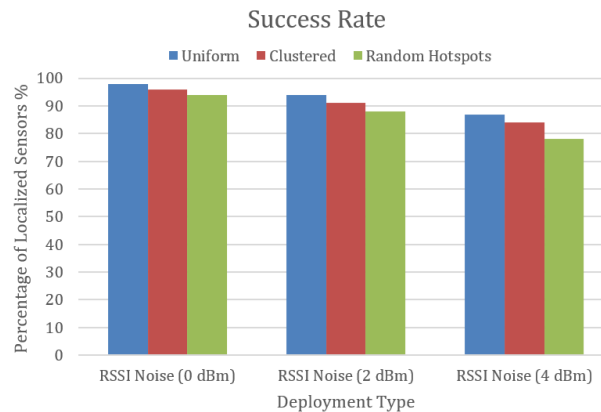


Figure 34: SQSPOA Success rate of node localization

## 3. Error Variability and Distribution

Figure 35 shows the boxplots of localization error for all combinations of deployment types and noise levels. As expected, both the median and the spread of error increase with noise. However, the interquartile range remains relatively narrow in uniform and clustered cases, indicating stable performance. In contrast, hotspot deployments exhibit higher variance, particularly at 4 dBm. These findings reinforce the claim that SQSPOA is resilient not only in average accuracy but also in consistency across node distributions and signal conditions.

## 4. Impact of Packet Loss on Localization Accuracy

Wireless sensor networks (WSNs) deployed in real-world environments are often subject to communication imperfections such as interference, fading, or congestion. These issues may lead to packet loss, which can degrade the reliability of received beacon messages and, consequently, the accuracy of localization. To assess the resilience of SQSPOA and baseline models under such imperfect conditions, we conducted simulations with increasing packet loss rates, ranging from 0% to 25%. During these tests, a percentage of anchor beacons were randomly dropped, simulating real-world wireless degradation. The localization error was then measured for each model to evaluate its robustness to communication unreliability.

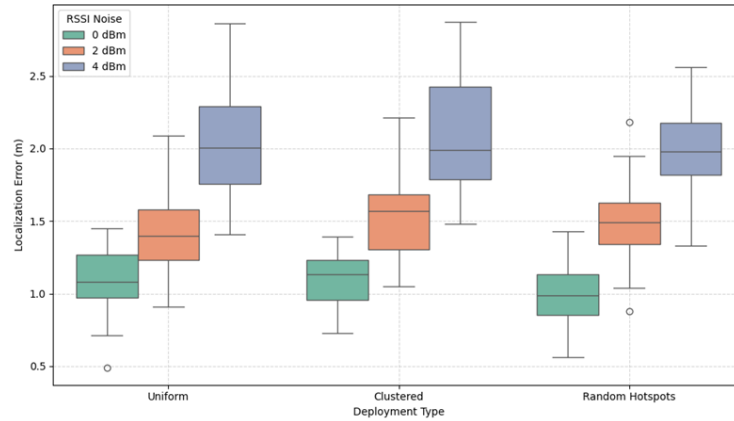


Figure 35: Distribution of localization errors

Figure 36 shows that localization error increases as packet loss rate rises. This trend is consistent across all models, yet the rate of degradation varies significantly. The proposed SQSPOA model demonstrates greater robustness, with a relatively slow error increase, maintaining acceptable accuracy (<1.5 m) even under 25% packet loss. On the other hand, legacy models such as NHexCurve and M-Curve experience sharper degradation, suggesting higher sensitivity to missing beacon information. These findings highlight the inherent resilience of SQSPOA’s trajectory and communication strategy, which provides better coverage redundancy and tolerance to beacon loss without relying on adaptive learning.

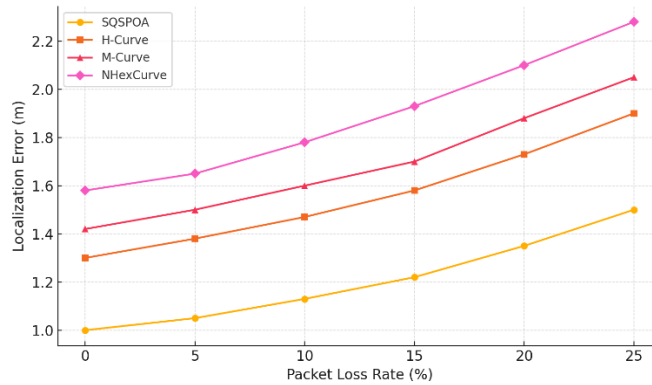


Figure 36: Localization Error vs. Packet Loss Rate

In summary, the results confirm that SQSPOA performs robustly under non-ideal deployment scenarios. The algorithm maintains high accuracy and coverage, even in the presence of noisy RSSI data and irregular sensor layouts. This highlights its potential for practical deployment in real-world WSNs where environment conditions are rarely ideal.

## 5 Conclusions

In this paper, we proposed a superior path planning model named SQSPOA for mobile anchor-assisted localization in wireless sensor networks. The proposed model estimates the location of sensor nodes with high accuracy by at least three non-collinear messages in the presence of different case studies of variable sizes obstacles. SQSPOA optimizes the number of beacon messages transmitted by the mobile anchor node, thus reducing times of broadcasting and receiving beacon messages by anchor and sensor nodes respectively which leads to reduction in power consumption for all nodes. SQSPOA ensures coverage of all area while giving a high percentage of localized sensor nodes due to covering all corners of the deployment field. The obstacle handling algorithm used by the proposed model ensures choosing the closest point while avoiding the obstacle (i.e. no more changes in the direction of the mobile anchor node), thereby saving energy consumption of the mobile anchor node. The simulation results comparison of the proposed model with three existing path planning models has confirmed the superiority of SQSPOA in terms of localization accuracy, percentage of localized sensor nodes and path length.

## 6 Future Work

In near future, we are planning to conduct more experiments to examine the proposed algorithm in the 3D environment. Also, we aim to extend SQSPOA to support dynamic environments with mobile obstacles or sensor nodes. This involves integrating adaptive path planning techniques and temporal beacon filtering mechanisms to ensure reliable localization in such complex settings. Moreover, future versions of the proposed algorithm could address the challenges associated with irregular-shaped obstacles by integrating shape-adaptive detour mechanisms and generalized obstacle modeling techniques. Future work may explore integrating adaptive and learning-based decision models with the deterministic framework of SQSPOA. In particular, extending the system to operate under dynamic and partially observable environments—as handled by DRL-based planners such as TD3—would significantly enhance its applicability in complex and unpredictable scenarios. While such treatment is beyond the scope of this work, it represents a promising direction for developing hybrid static–adaptive localization strategies that balance coverage reliability with environment-driven adaptability.

### Acknowledgements

The work presented in this paper was supported by the Deanship of Graduate Studies and Scientific Research at Jouf University under grant No. (DGSSR-2024-02-02111). Any opinions, findings and conclusions or recommendations expressed in this publication are those of the authors and do not necessarily reflect the views of the Deanship of Graduate Studies and Scientific Research at Jouf University.

### References

[Achroufene, 23] Achroufene, A.: RSSI-based geometric localization in wireless sensor networks, *Journal of Supercomputing*, vol. 79, 5615–5642, 2023, <https://doi.org/10.1007/s11227-022-04887-5>.

- [Ahmad, 24] Ahmad, N. S.: Recent advances in WSN-based indoor localization: A systematic review of emerging technologies, methods, challenges, and trends, *IEEE Access*, vol. 12, 180674–180714, 2024, <https://ieeexplore.ieee.org/abstract/document/10772114>.
- [Alhmiedat, 23] Alhmiedat, T.: Fingerprint-Based Localization Approach for WSN Using Machine Learning Models, *Applied Sciences*, vol. 13, no. 5, article 3037, 2023, <https://www.mdpi.com/2076-3417/13/5/3037>
- [Alomari, 18] Alomari, A., Comeau, F., Phillips, W., Aslam, N.: New Path Planning Model for Mobile Anchor-Assisted Localization in Wireless Sensor Networks, *Wireless Networks*, vol. 24, 2589–2607, 2018, <https://doi.org/10.1007/s11276-017-1493-2>
- [Buehrer, 18] Buehrer, R. M., Wymeersch, H., Vaghefi, R. M.: Collaborative sensor network localization: Algorithms and practical issues, *Proceedings of the IEEE*, vol. 106, no. 6, 1089–1114, 2018, <https://ieeexplore.ieee.org/document/8359446>
- [Camp, 02] Camp, T., Boleng, J., Davies, V.: A Survey of Mobility Models for Ad Hoc Network Research, *Wireless Communications and Mobile Computing*, vol. 2, no. 5, 483–502, 2002, <https://doi.org/10.1002/wcm.72>
- [Chang, 09a] Chang, C. Y., Chang, C. T., Chen, Y. C., Chang, H. R.: Obstacle-Resistant Deployment Algorithms for Wireless Sensor Networks, *IEEE Transactions on Vehicular Technology*, vol. 58, no. 6, 2925–2941, 2009, <https://doi.org/10.1109/TVT.2008.2010619>
- [Chang, 09b] Chang, C. Y., Sheu, J. P., Chen, Y. C., Chang, S. W.: An Obstacle-Free and Power-Efficient Deployment Algorithm for Wireless Sensor Networks, *IEEE Transactions on Systems, Man, and Cybernetics - Part A: Systems and Humans*, vol. 39, no. 4, 795–806, 2009, <https://doi.org/10.1109/TSMCA.2009.2014389>
- [Chen, 21] Chen, D., Li, S., Wu, Q.: A Novel Supertwisting Zeroing Neural Network with Application to Mobile Robot Manipulators, *IEEE Transactions on Neural Networks and Learning Systems*, vol. 32, no. 4, 1776–1787, 2021, <https://doi.org/10.1109/TNNLS.2020.2991088>
- [Erdemir, 18] Erdemir, E., Tuncer, T. E.: Path planning for mobile-anchor based wireless sensor network localization: Static and dynamic schemes, *Ad Hoc Networks*, vol. 77, 1–10, 2018, <https://doi.org/10.1016/j.adhoc.2018.04.005>
- [Fawad, 23] Fawad, M., Khan, M. Z., Ullah, K., Alasmary, H., Shehzad, D., Khan, B.: Enhancing Localization Efficiency and Accuracy in Wireless Sensor Networks, *Sensors*, vol. 23, no. 5, article 2796, 2023, <https://www.mdpi.com/1424-8220/23/5/2796>
- [Halder, 16] Halder, S., Ghosal, A.: A survey on mobile anchor assisted localization techniques in wireless sensor networks, *Wireless Networks*, vol. 22, 2317–2336, 2016, <https://doi.org/10.1007/s11276-015-1101-2>
- [Han, 16] Han, G., Jiang, J., Zhang, C., Duong, T. Q., Guizani, M., Karagiannidis, G. K.: A survey on mobile anchor node assisted localization in wireless sensor networks, *IEEE Communications Surveys & Tutorials*, vol. 18, no. 3, 2220–2243, 2016, <https://ieeexplore.ieee.org/abstract/document/7438736>
- [Han, 13] Han, G., Xu, H., Jiang, J., Shu, L., Hara, T., Nishio, S.: Path Planning Using a Mobile Anchor Node Based on Trilateration in Wireless Sensor Networks, *Wireless Communications and Mobile Computing*, vol. 13, no. 14, 1324–1336, 2013, <https://doi.org/10.1002/wcm.1192>
- [Huang, 07] Huang, R., Zaruba, G. V.: Static Path Planning for Mobile Beacons to Localize Sensor Networks, *Proc. IEEE Int. Conf. on Pervasive Computing and Communications Workshops (PerComW'07)*, 323–330, 2007, <https://doi.org/10.1109/PERCOMW.2007.109>

- [Kannadasan, 20] Kannadasan, K., Edla, D. R., Kongara, M. C., Kuppili, V. B.: M-Curves Path Planning Model for Mobile Anchor Node and Localization of Sensor Nodes Using Dolphin Swarm Algorithm, *Wireless Networks*, vol. 26, no. 4, 2769–2783, 2020, <https://doi.org/10.1007/s11276-019-02032-4>
- [Koutsonikolas, 07] Koutsonikolas, D., Das, S. M., Hu, Y. C.: Path Planning of Mobile Landmarks for Localization in Wireless Sensor Networks, *Computer Communications*, vol. 30, no. 13, 2577–2592, 2007, <https://doi.org/10.1016/j.comcom.2007.05.048>
- [Kulkarni, 23] Kulkarni, V. R.: Comparative analysis of static and mobile anchors in sensor localization, 2023 International Conference on Device Intelligence, Computing and Communication Technologies (DICCT), Dehradun, India, 115–120, 2023, <https://ieeexplore.ieee.org/abstract/document/10110135>
- [Liu, 22] Liu, W., Luo, X., Wei, G., Liu, H.: Node localization algorithm for wireless sensor networks based on static anchor node location selection strategy, *Computer Communications*, vol. 192, 289–298, 2022.
- [Mohajer, 25] Mohajer, A., Hajipour, J., Leung, V. C. M.: Dynamic Offloading in Mobile Edge Computing with Traffic-Aware Network Slicing and Adaptive TD3 Strategy, *IEEE Communications Letters*, vol. 29, no. 1, 95–99, Jan. 2025, <https://doi.org/10.1109/LCOMM.2024.3501956>
- [Naguib, 21] Naguib, A. M., Ali, S.: A Novel Static Path Planning Method for Mobile Anchor-Assisted Localization in Wireless Sensor Networks, *International Journal of Sensors Wireless Communications and Control*, vol. 11, no. 4, 482–493, 2021, <https://doi.org/10.2174/2210327910999200723164502>
- [Naguib, 24] Naguib, A.: Outstanding Framework for Simulating and Generating Anchor Trajectory in Wireless Sensor Networks, *International Journal of Computer Networks and Communications*, vol. 16, no. 6, 21–39, 2024, <https://airconline.com/abstract/ijcnc/v16n6/16624enc02.html>
- [Nguyen, 19] Nguyen, N. M., Tran, L. C., Safaei, F., Phung, S. L., Vial, P., Huynh, N., Cox, A., Harada, T., Barthelemy, J.: Performance evaluation of non-GPS based localization techniques under shadowing effects, *Sensors*, vol. 19, 2633, 2019, <https://doi.org/10.3390/s19112633>
- [NS-3, 24] NS-3 Consortium: NS-3 Network Simulator, 2024, <https://www.nsnam.org>
- [Numan et al., 20] Numan, M., et al.: A systematic review on clone node detection in static wireless sensor networks, *IEEE Access*, vol. 8, 65450–65461, 2020, <https://ieeexplore.ieee.org/abstract/document/9046044>
- [Oliveira, 23] Oliveira, L. L. de, Eisenkraemer, G. H., Carara, E. A., Martins, J. B., Monteiro, J.: Mobile Localization Techniques for Wireless Sensor Networks: Survey and Recommendations, *ACM Transactions on Sensor Networks*, vol. 19, no. 2, 1–39, 2023, <https://doi.org/10.1145/3561512>
- [Peng, 19] Peng, Z., Wang, J., Han, Q. L.: Path-Following Control of Autonomous Underwater Vehicles Subject to Velocity and Input Constraints via Neurodynamic Optimization, *IEEE Transactions on Industrial Electronics*, vol. 66, no. 11, 8724–8732, 2019, <https://doi.org/10.1109/TIE.2018.2885726>
- [Phoemphon, 24] Phoemphon, S.: Distance estimation using the relative densities and connectivity of sensor nodes for wireless sensor network localization, *IEEE Access*, vol. 12, 138881–138903, 2024, <https://ieeexplore.ieee.org/abstract/document/10683693>

- [Qu et al., 13] Qu, H., Hou, G., Guo, Y., Wang, N., Guo, Z.: Localization with single stationary anchor for mobile node in wireless sensor networks, *International Journal of Distributed Sensor Networks*, vol. 9, no. 4, 2013, <https://journals.sagepub.com/doi/10.1155/2013/212806>
- [Rezazadeh, 14] Rezazadeh, J., Moradi, M., Ismail, A. S., Dutkiewicz, E.: Superior Path Planning Mechanism for Mobile Beacon-Assisted Localization in Wireless Sensor Networks, *IEEE Sensors Journal*, vol. 14, no. 9, 3052–3064, 2014, <https://doi.org/10.1109/JSEN.2014.2322958>
- [Sabale, 21] Sabale, K., Mini, S.: Localization in wireless sensor networks with mobile anchor node path planning mechanism, *Information Sciences*, vol. 579, 648–666, 2021, <https://doi.org/10.1016/j.ins.2021.08.004>.
- [Shahal, 23] Shahal, B. A., Abdullah, M. N.: A Review of Localization Algorithms Based on Software Defined Networking Approach in Wireless Sensor Network, *Measurement: Sensors*, vol. 27, article 100772, 2023, <https://doi.org/10.1016/j.measen.2023.100772>
- [Singh, 17] Singh, M., Khilar, P. M.: Mobile beacon-based range free localization method for wireless sensor networks, *Wireless Networks*, vol. 23, 1285–1300, 2017, <https://doi.org/10.1007/s11276-016-1227-x>
- [Singh, 18] Singh, P., Khosla, A., Kumar, A., Khosla, M.: Optimized localization of target nodes using single mobile anchor node in wireless sensor network, *AEU - International Journal of Electronics and Communications*, vol. 91, 55–65, 2018, <https://doi.org/10.1016/j.aeue.2018.04.024>
- [Singh, 15] Singh, S. P., Sharma, S. C.: Range free localization techniques in wireless sensor networks: A review, *Procedia Computer Science*, vol. 57, 7–16, 2015, <https://doi.org/10.1016/j.procs.2015.07.357>
- [Upadhyay, 22] Upadhyay, V., Roy, K., Balakrishnan, M.: Beacon placement and signal strength estimation to improve localization coverage and accuracy, 2022 IEEE 12th International Conference on Indoor Positioning and Indoor Navigation (IPIN), Beijing, China, 1–8, 2022, <https://ieeexplore.ieee.org/abstract/document/9918130>
- [Wu, 20] Wu, Q., Chen, Z., Wang, L., Lin, H., Jiang, Z., Li, S., Chen, D.: Real-Time Dynamic Path Planning of Mobile Robots: A Novel Hybrid Heuristic Optimization Algorithm, *Sensors*, vol. 20, no. 1, article 188, 2020, <https://doi.org/10.3390/s20010188>
- [Yang, 10] Yang, Z., Liu, Y.: Quality of Trilateration: Confidence-Based Iterative Localization, *IEEE Transactions on Parallel and Distributed Systems*, vol. 21, no. 5, 631–640, 2010, <https://doi.org/10.1109/TPDS.2009.90>
- [Yang, 25] Yang, J., Mohajer, A.: Multi-Objective Constellation Optimization and Dynamic Link Utilization for Sustainable Information Delivery Using PD-NOMA Deep Reinforcement Learning, *Wireless Networks*, vol. 31, 1839–1859, 2025, <https://doi.org/10.1007/s11276-024-03834-x>
- [Yildiz, 21] Yildiz, D., Karagol, S.: Path Planning for Mobile-Anchor Based Wireless Sensor Networks Localization: Obstacle-Presence Schemes, *Sensors*, vol. 21, no. 11, article 3697, 2021, <https://doi.org/10.3390/s21113697>
- [Zhou, 24] Zhou, G., Mohajer, A.: Blind Reconfigurable Intelligent Surfaces for Dynamic Offloading in Fixed-NOMA Mobile Edge Networks, *International Journal of Sensor Networks*, vol. 46, no. 3, 142–160, 2024, <https://doi.org/10.1504/IJSNET.2024.142517>